Azimuthal anisotropy in elastic and equivalent media

Sitamai Ajiduah*, Gary Margrave and Patrick Daley

Outline

- Theory
  - Schoenberg and Muir Equivalent model
  - Shear-wave birefringence
- Workflow
- Results
  - Ruger modeling
  - Numerical dataset modeling of elastic and equivalent media
  - AVAZ analysis
  - TVAZ analysis
- Conclusions

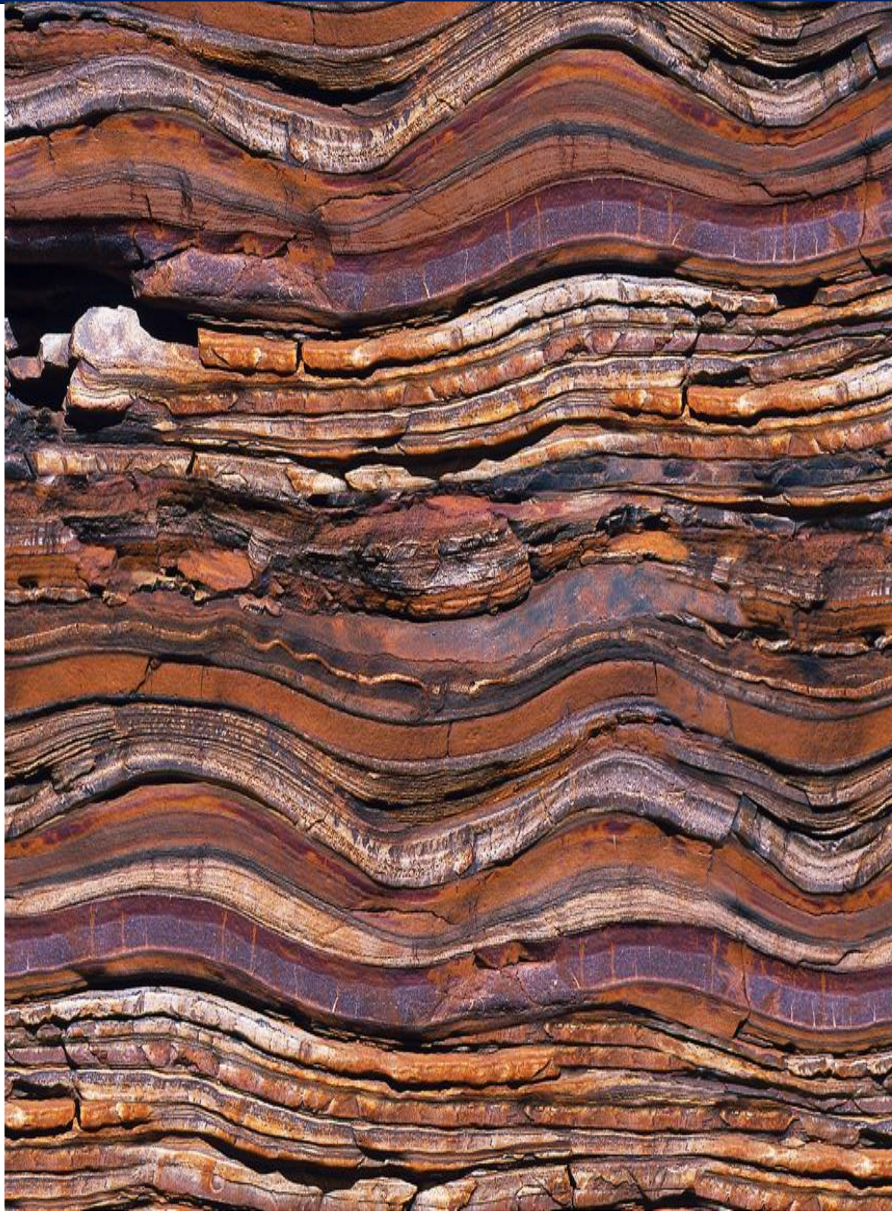

Schoenberg and Muir Theory

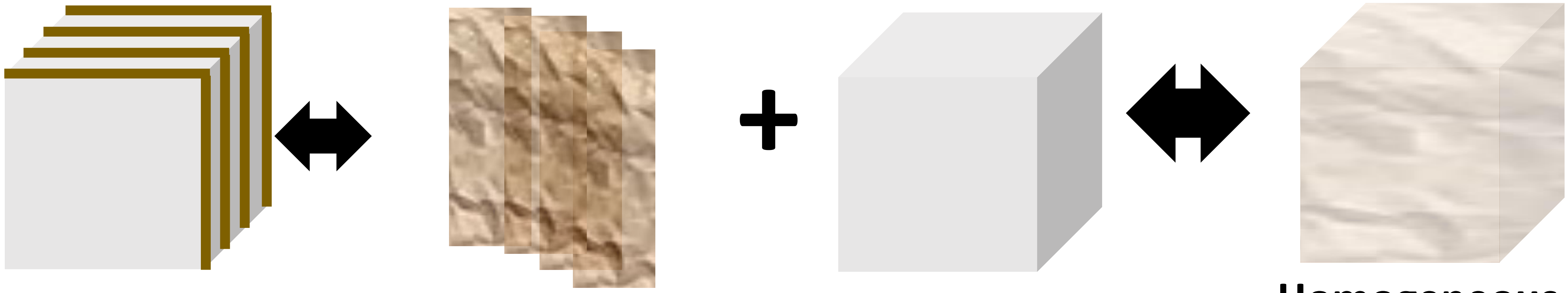

Heterogeneous fractured medium.

Fractures

Homogeneous host medium

Homogeneous anisotropic equivalent medium (Schoenberg, (1989)

$$\boldsymbol{G} = \boldsymbol{G}_{\boldsymbol{f}} + \boldsymbol{G}_{\boldsymbol{b}}$$

Group set of fractured medium

Group set of fracture properties

Group set of unfractured background properties

Criteria: (i). Backus averaging criteria

(ii). Linear slip conditions or imperfectly bounded interface.

Schoenberg and Muir Theory

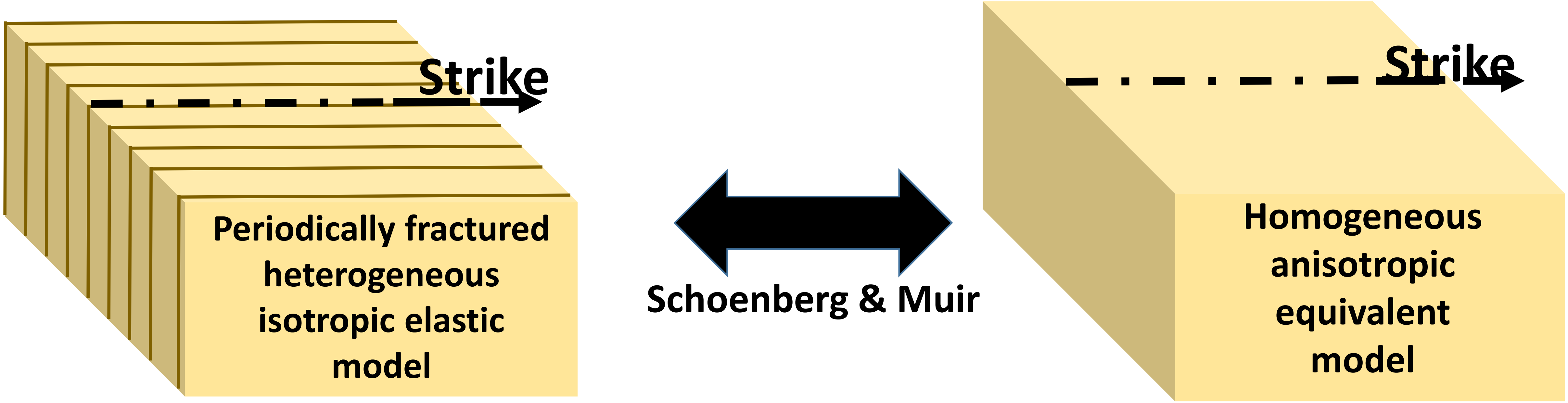

$$\overline{C}_{NN} = \langle \overline{C}_{NN}^{-1} \rangle^{-1}$$

$$\overline{C}_{TN} = \langle C_{TN} C_{NN}{}^{-1} \rangle \overline{C}_{NN}$$

$$\overline{C}_{TT} = \langle C_{TT} \rangle - \langle C_{TN} C_{NN}{}^{-1} C_{NT} \rangle + \overline{C}_{TN} \langle \overline{C}_{NN}^{-1} C_{NT} \rangle$$

$$\{V_{p\,h}, V_{s\,h}, \rho_{h}, V_{p\,f}, V_{s\,f}, \rho_{f}\}$$

$$\{V_{p0}, V_{s0}, \rho^{e}, \epsilon^{e}, \gamma^{e}, \varphi\}$$

Shear wave birefringence

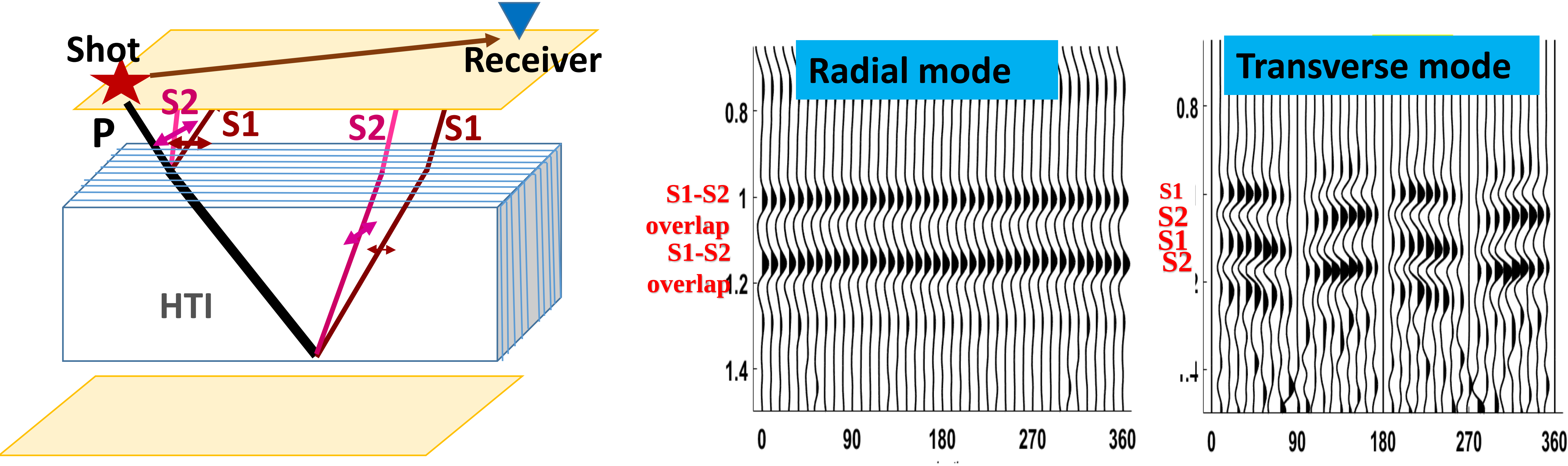

- **Shear-wave splits into fast S1 and slow S2 modes**
- **Shear wave splitting effects: Sinusoidal event seen on radial dataset; Mode separation and polarity reversal seen on transverse component.**

Vertically fractured heterogeneous elastic model. (Isotropic host + fracture)
$V_{p\,h}, V_{s\,h}, \rho_{h}, V_{p\,f}, V_{s\,f}, \rho_{f}$

Homogeneous equivalent model Schoenberg (1989)
$\{C_{ij}, V_{p0}, V_{s0}, \rho^{e}, \epsilon^{e}, \gamma^{e}, \varphi\}$

Forward modeling

Band –Pass filtering

Rotate dataset from Z,X,Y to Z,R,T

Create azimuthal-offset dataset

Ruger Amplitudes

Compare

Interpretation

Workflow: Seismic Acquisition

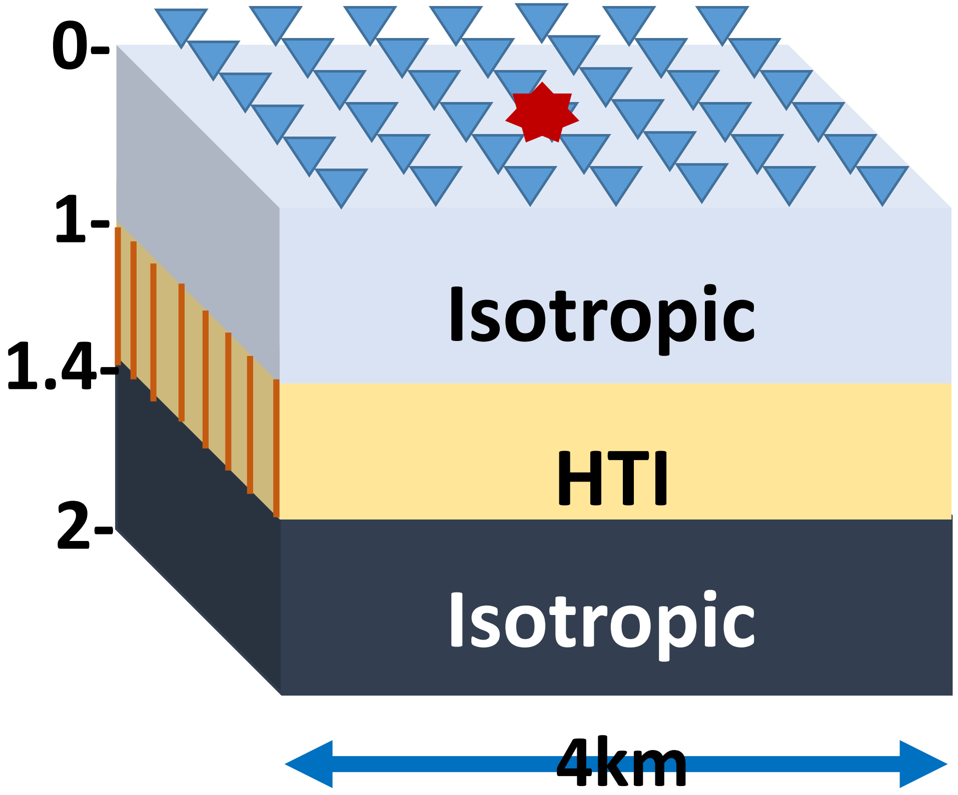

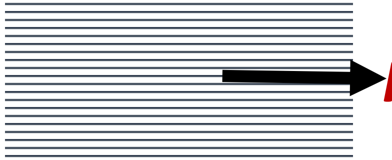

	Heterogeneous elastic model	*Homogeneous equivalent model*
Layer1	$Vp = 3500, Vs = 2140$, $\rho = 2200$	*same*
HTI Layer	$Vp_1 = 4700$, $Vs_2 = 3980$, $\rho_1 = 2500$, $Vp_2 = 4210$, $Vs_2 = 2430$, $\rho_2 = 2300$	$Vp_0 = 4438$, $Vs_0 = 2746$, $\rho^e = 2401$, $\epsilon^e = .0034$, $\gamma^e = .0607$, $\delta^e = -.0545$
Layer3	$Vp = 5000, Vs = 3300$, $\rho = 2900$	*same*

Acquisition

- 3D-3C acquisition WAZ
- Orthogonal design
- Finite difference
- Explosive P source.
- 40m source & receiver depth
- Source frequency is 15hz

Constant azimuth radial scans and constant offset azimuthal scans

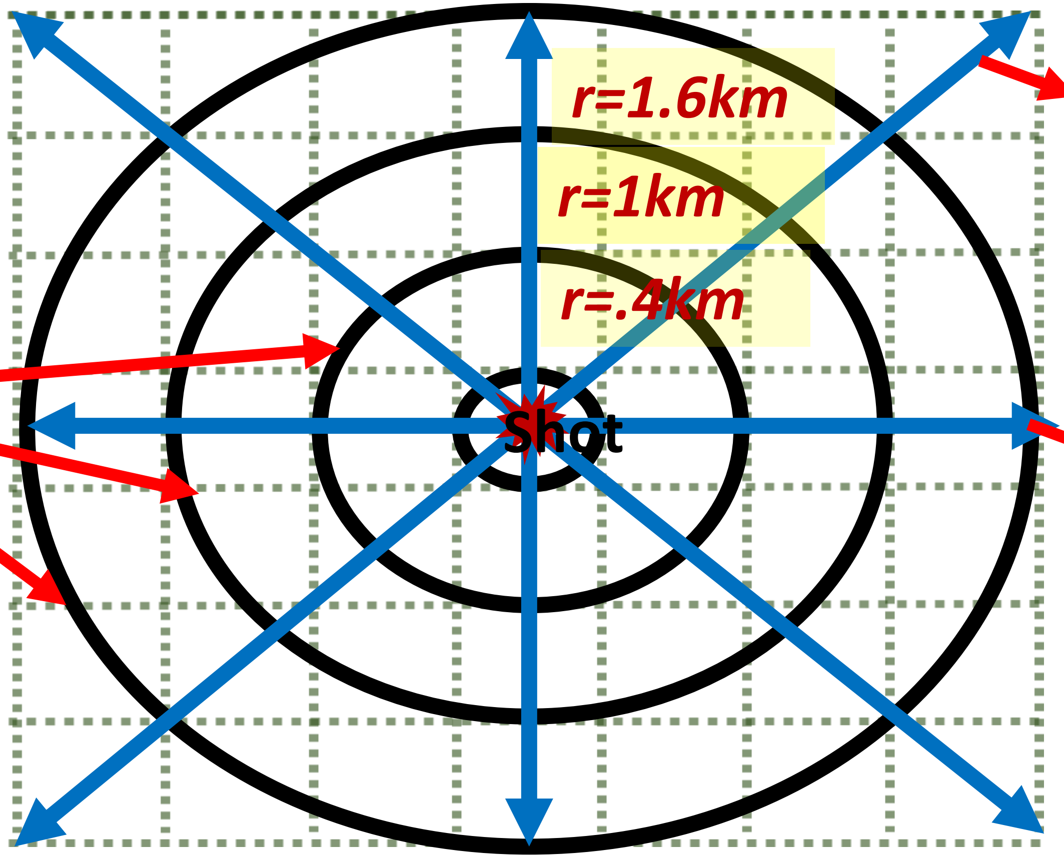

Constant offset azimuthal scans

45^0 constant azimuth radial scan

0^0 constant azimuth radial scan

Result: Analytical results from Ruger approx. -TOP OF HTI

Fracture strike direction

$REFL_{PP}$ *from TOP of HTI*

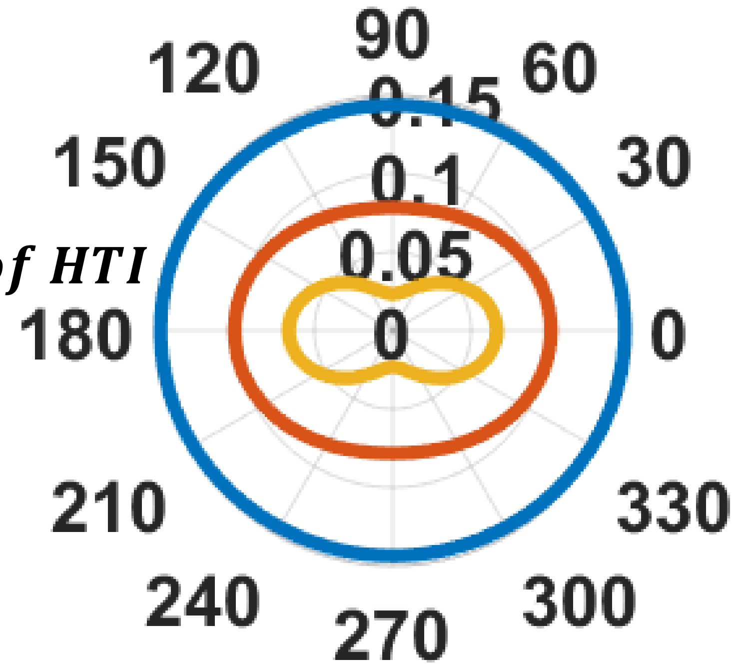

r=.4 r=1 r=1.6 km

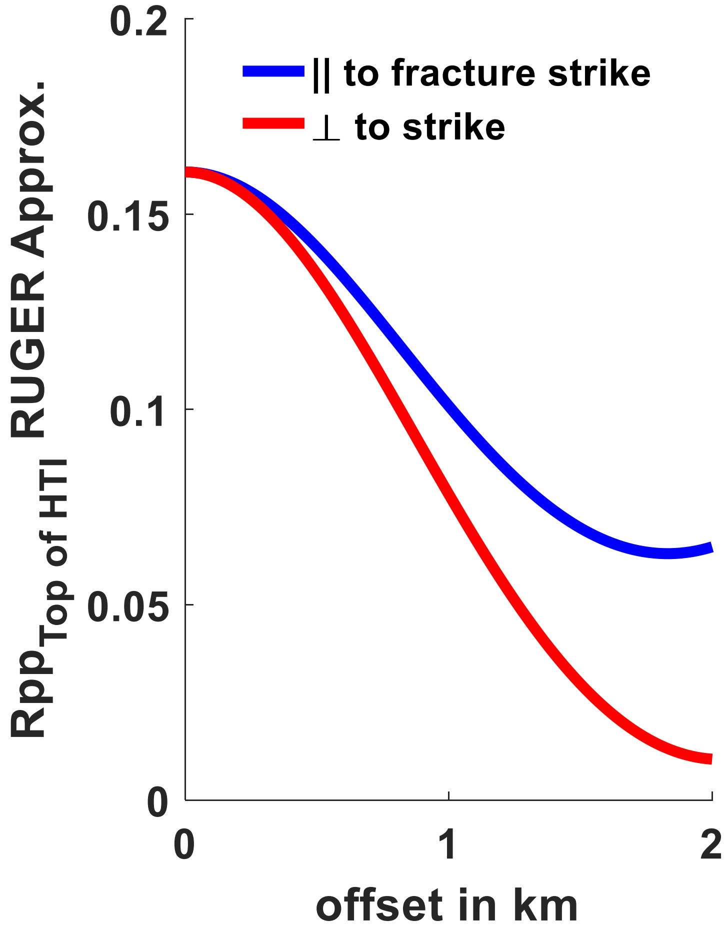

Identifying typical PP, PPpp, PS and PPps

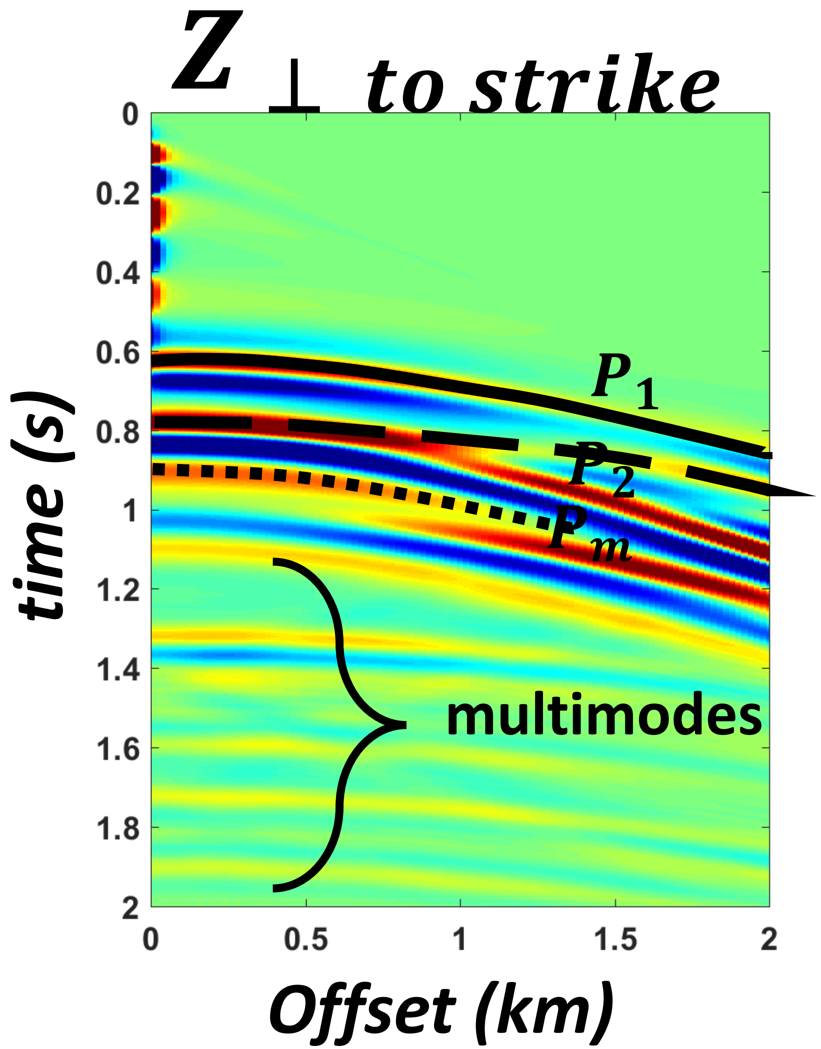

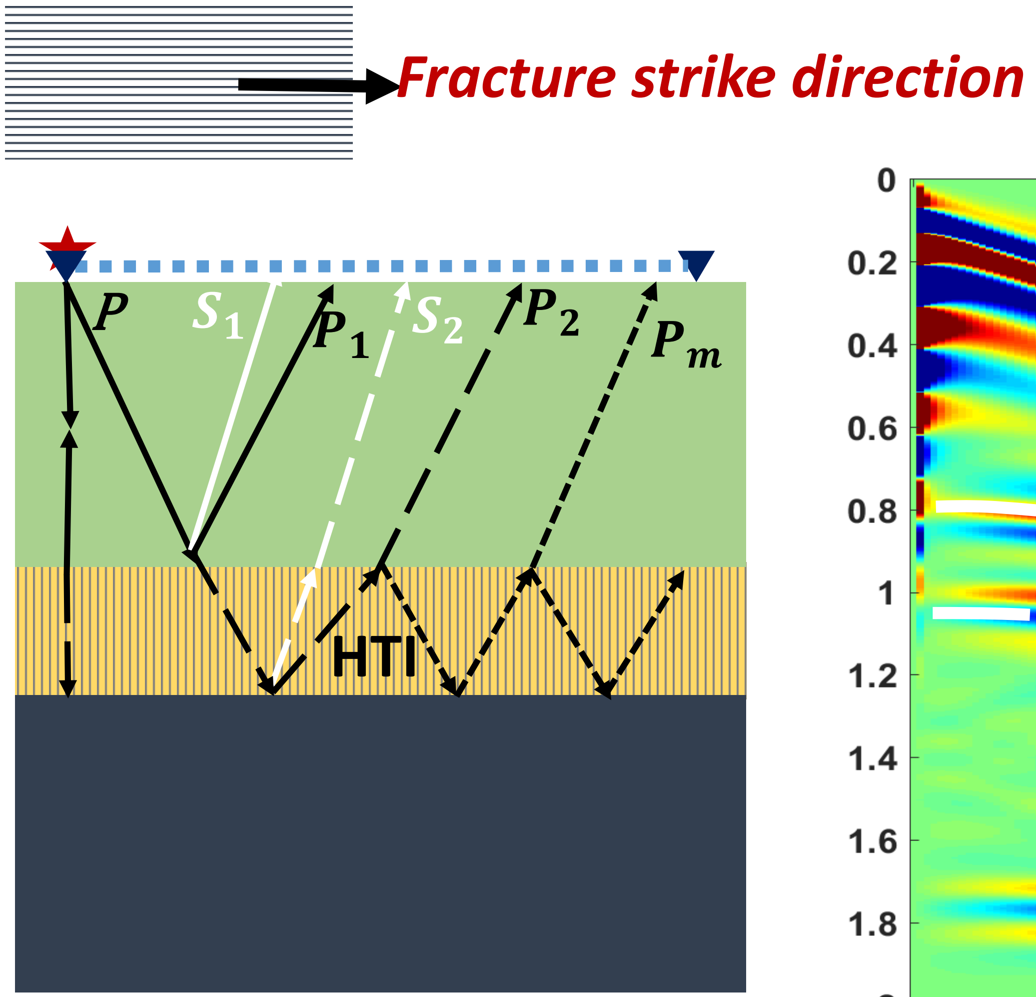

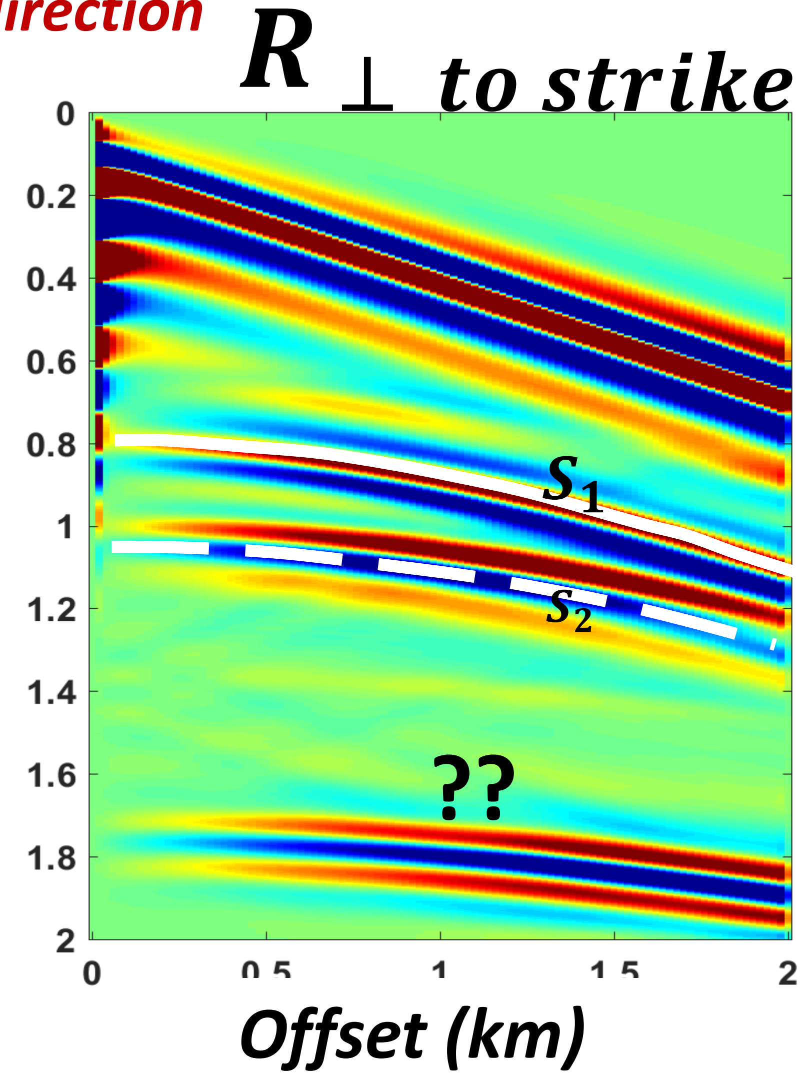

Example: Vertical dataset

Elastic modeling

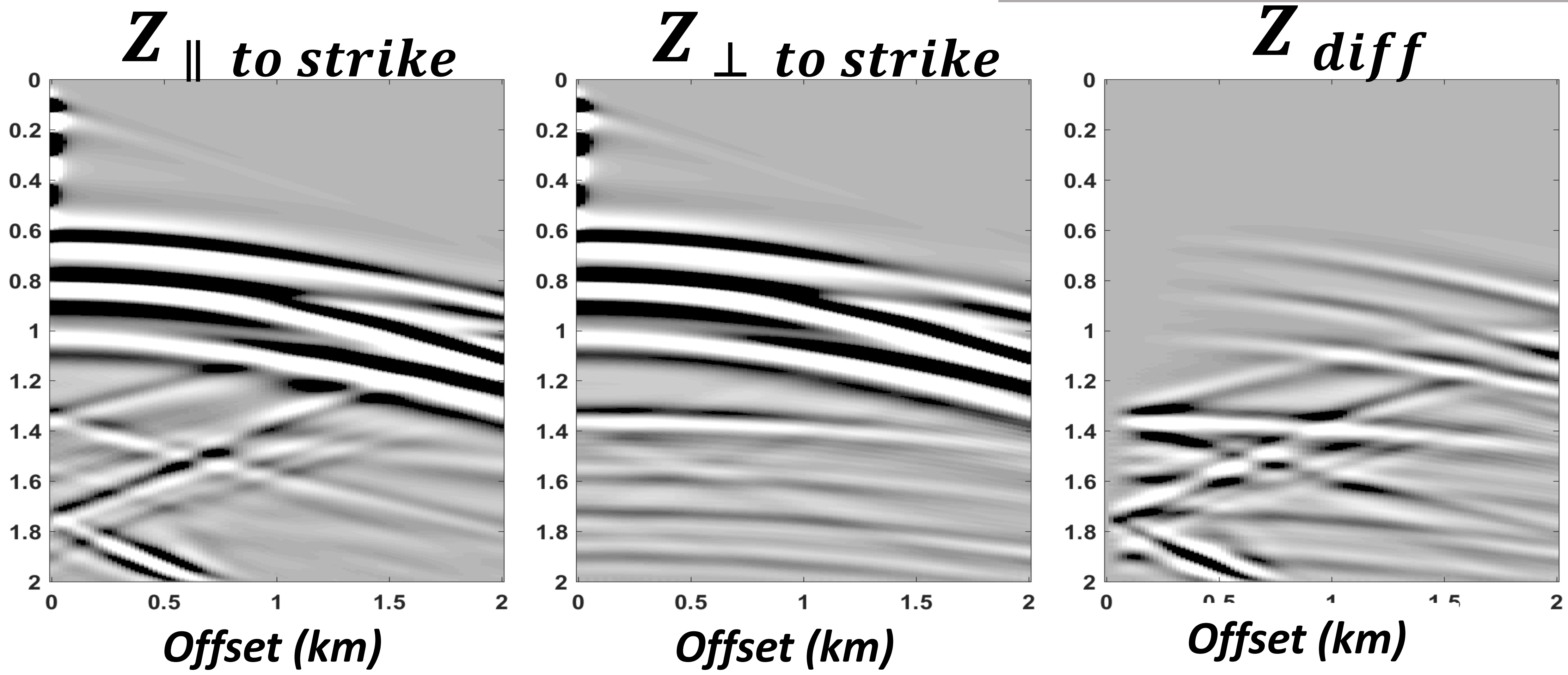

Example: Vertical component dataset

Equivalent modeling

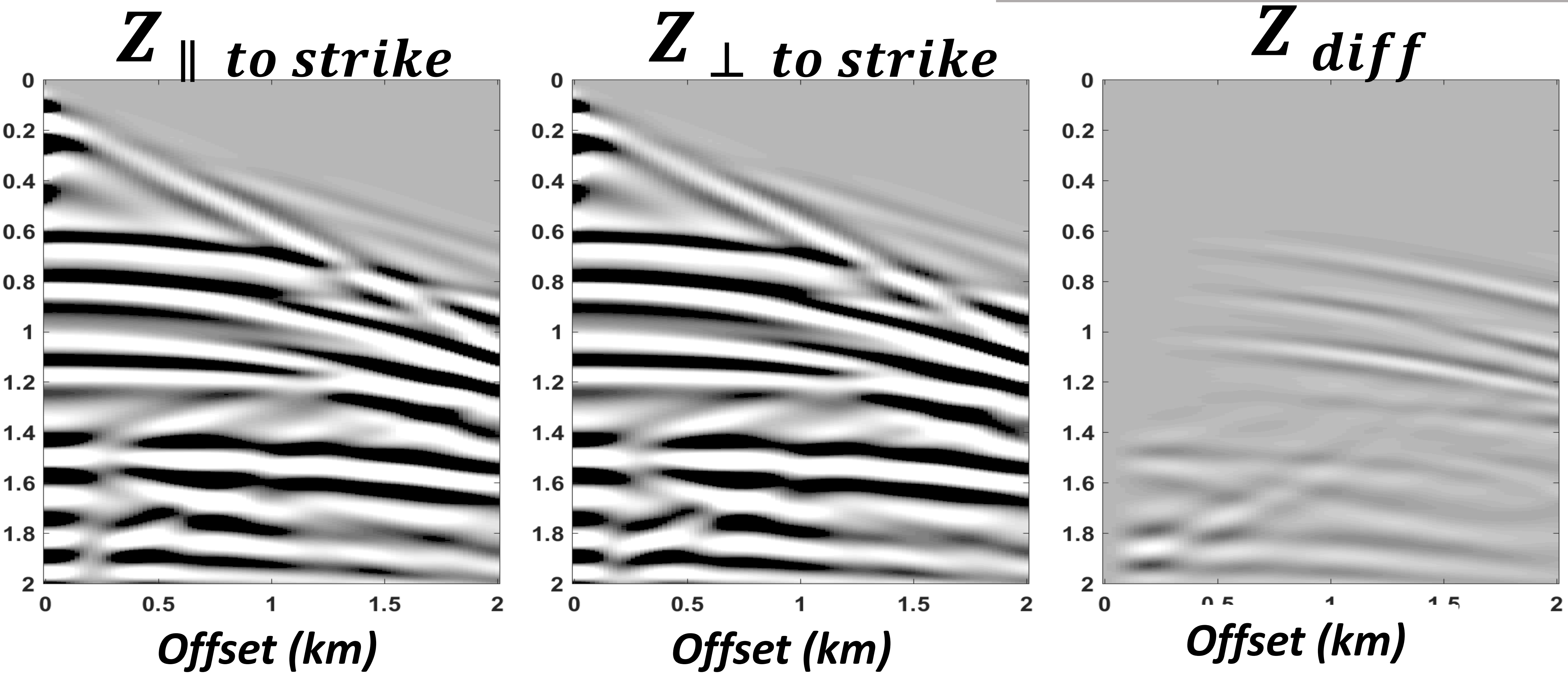

Example: Radial component dataset

Elastic modeling

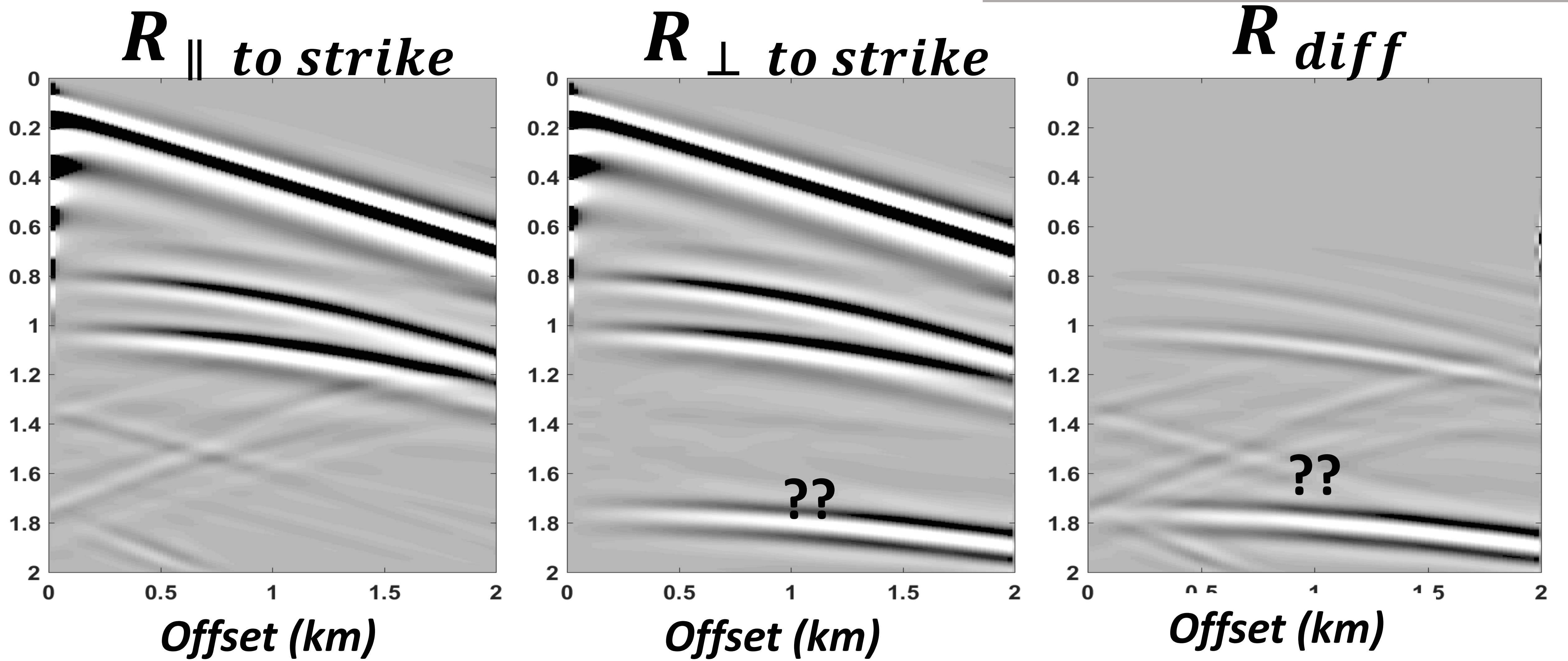

Example: Radial component dataset

Equivalent modeling

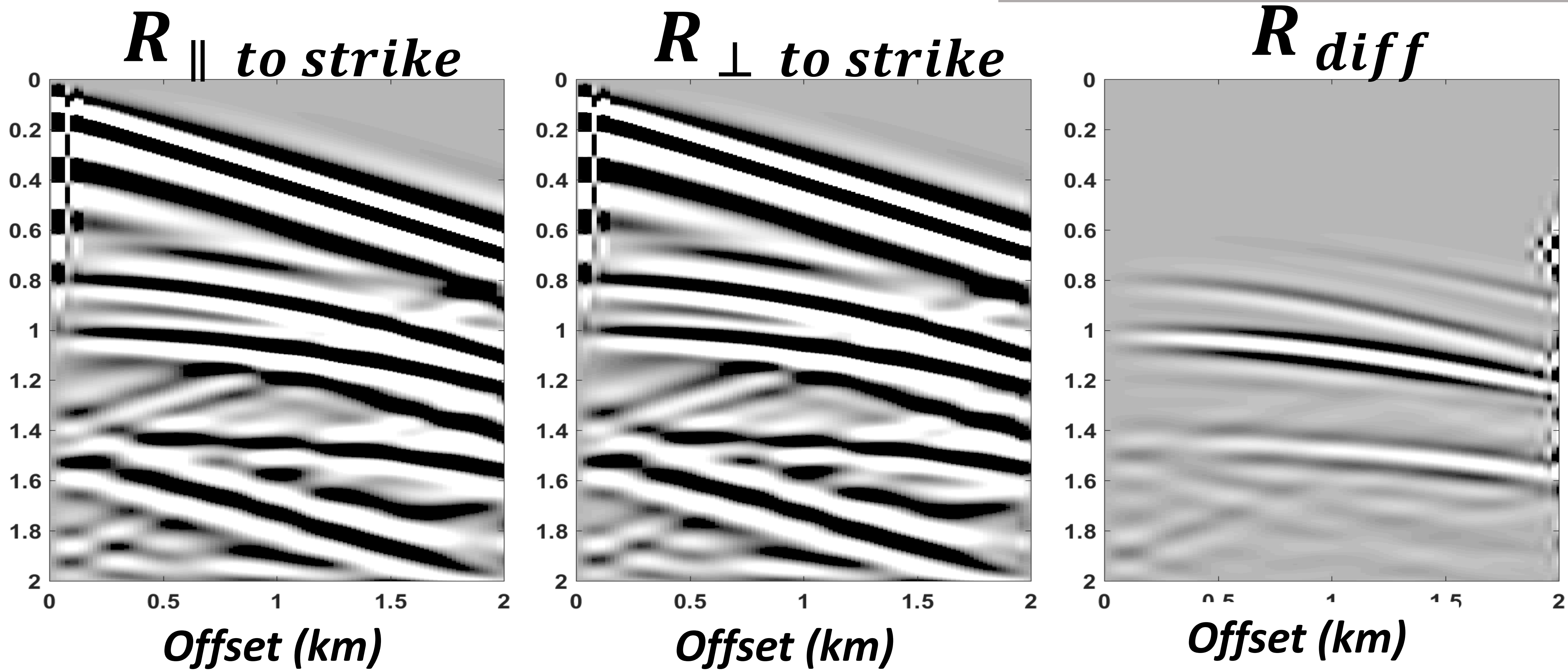

Example: Transverse component dataset

Elastic modeling

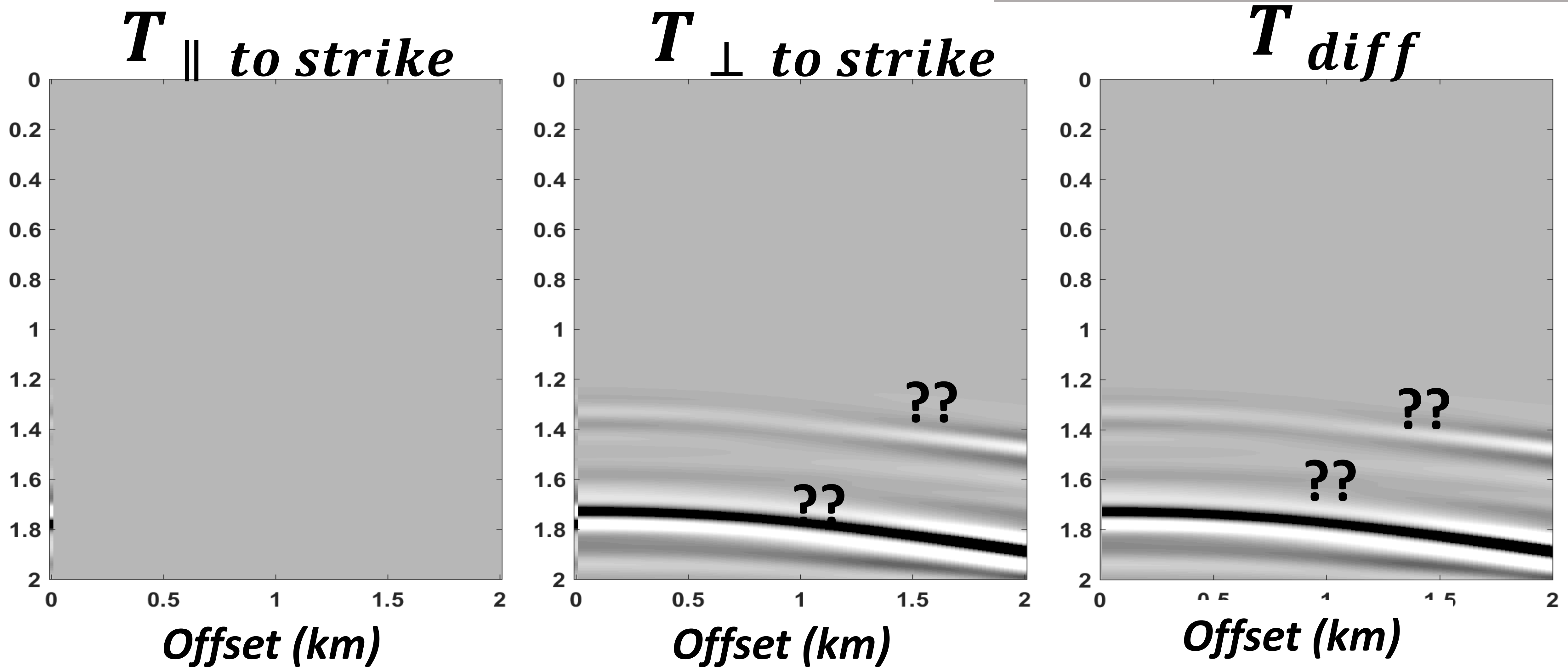

Example: Transverse component dataset

Equivalent modeling

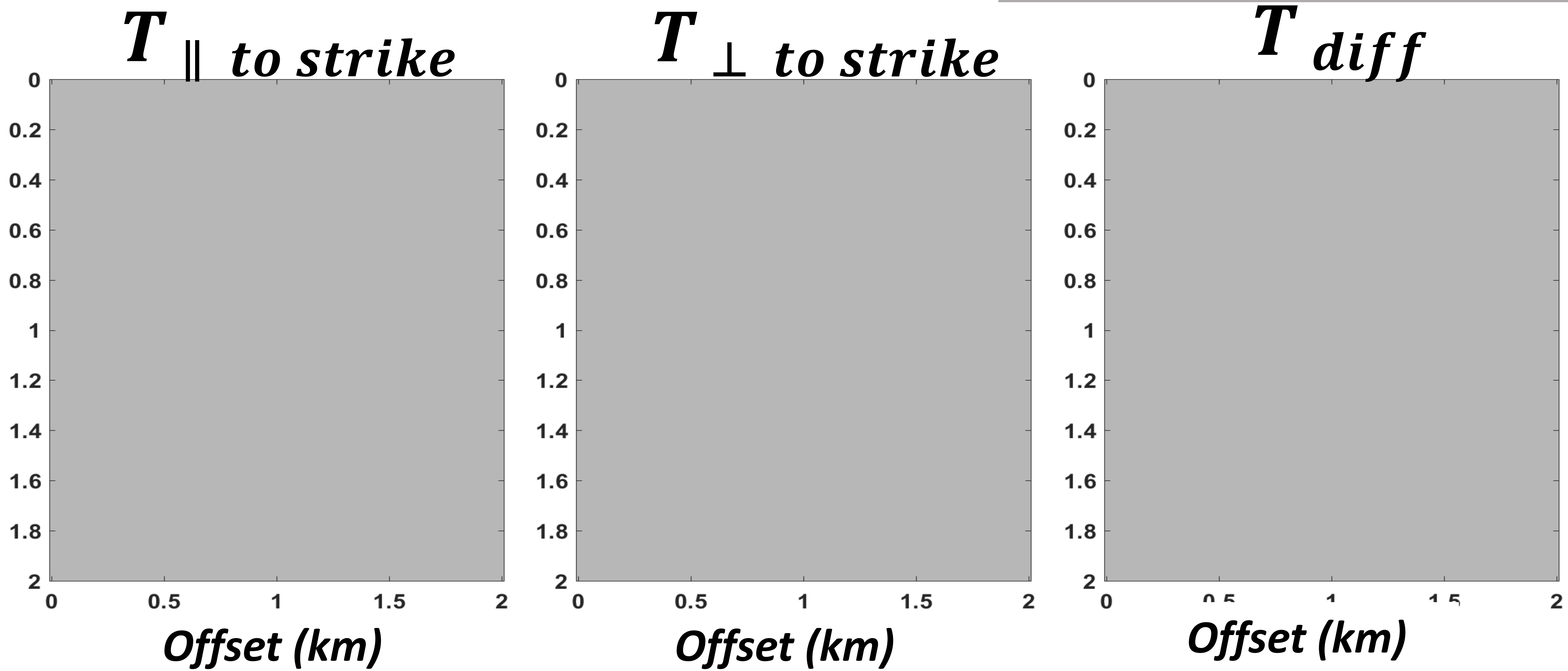

Example: Constant-azimuth Radial Scans

$Z_{(t,r,\varphi)}$

elastic modeling

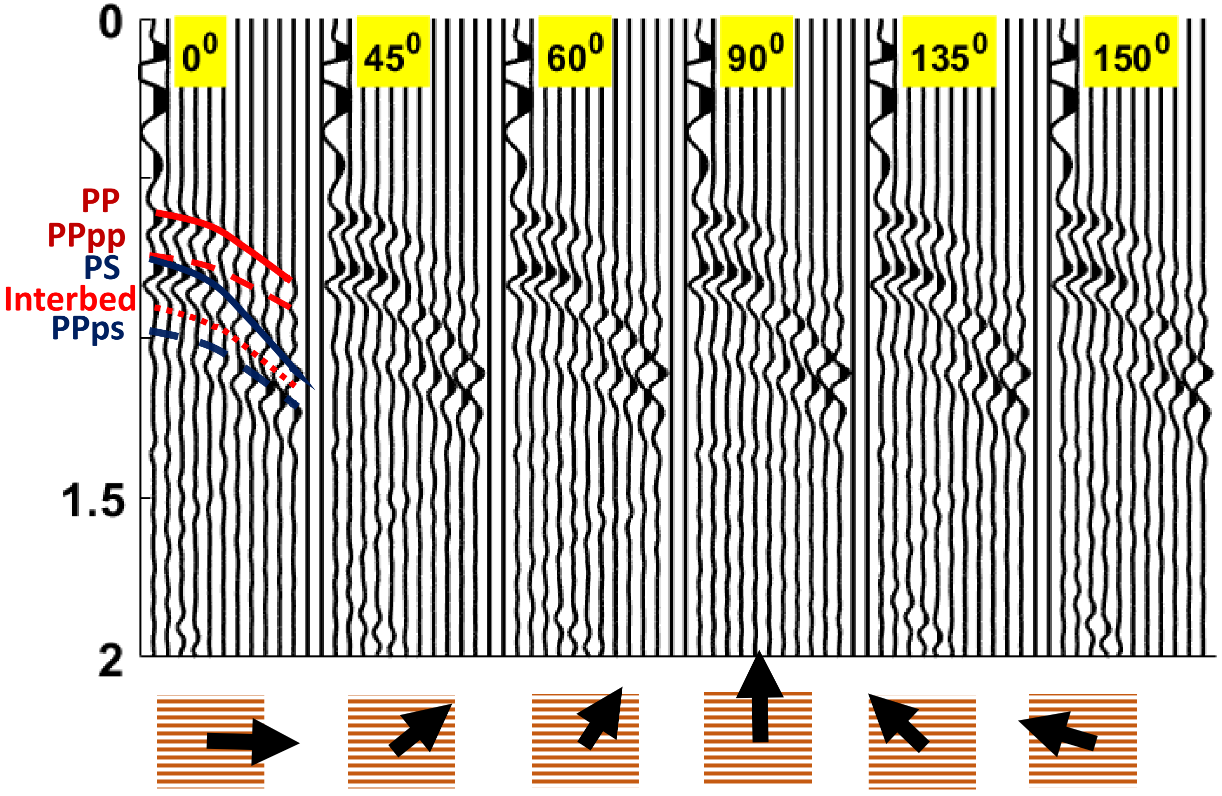

$Z_{(t,r,\varphi)}$

equivalent modeling

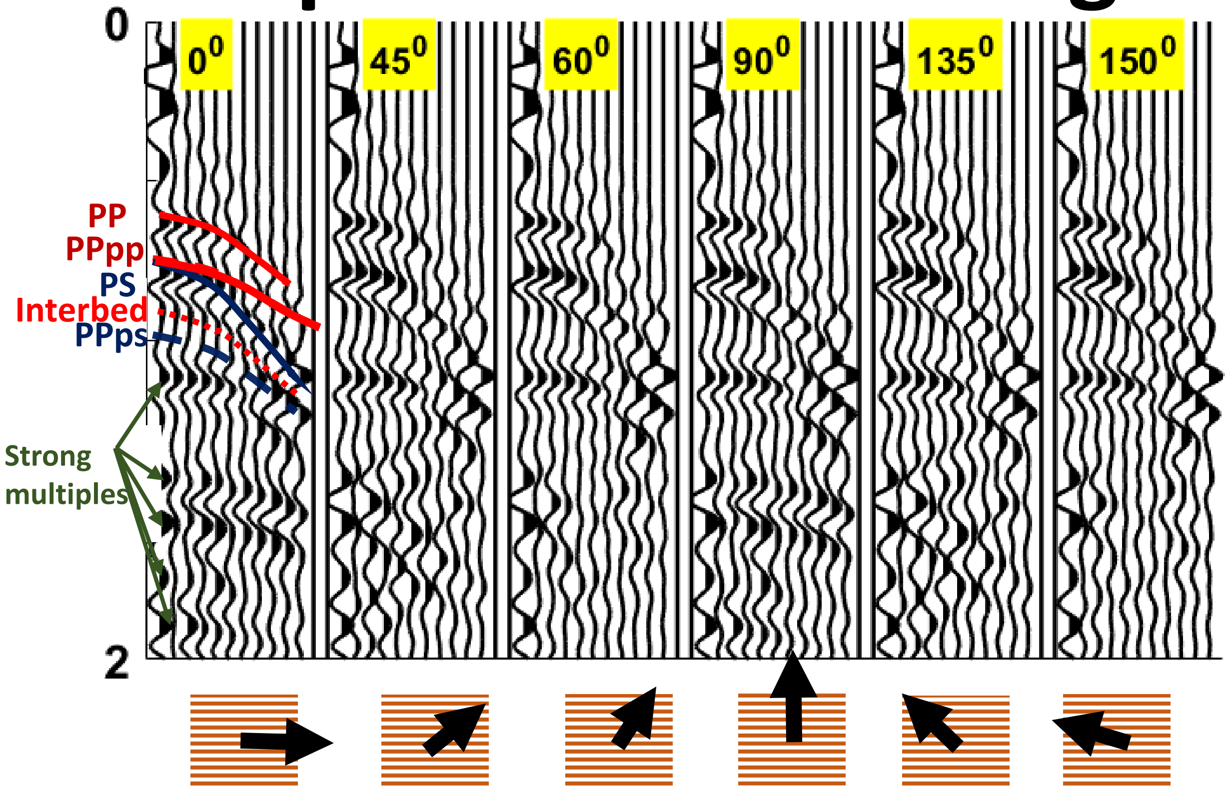

Example: Constant-azimuth Radial Scans

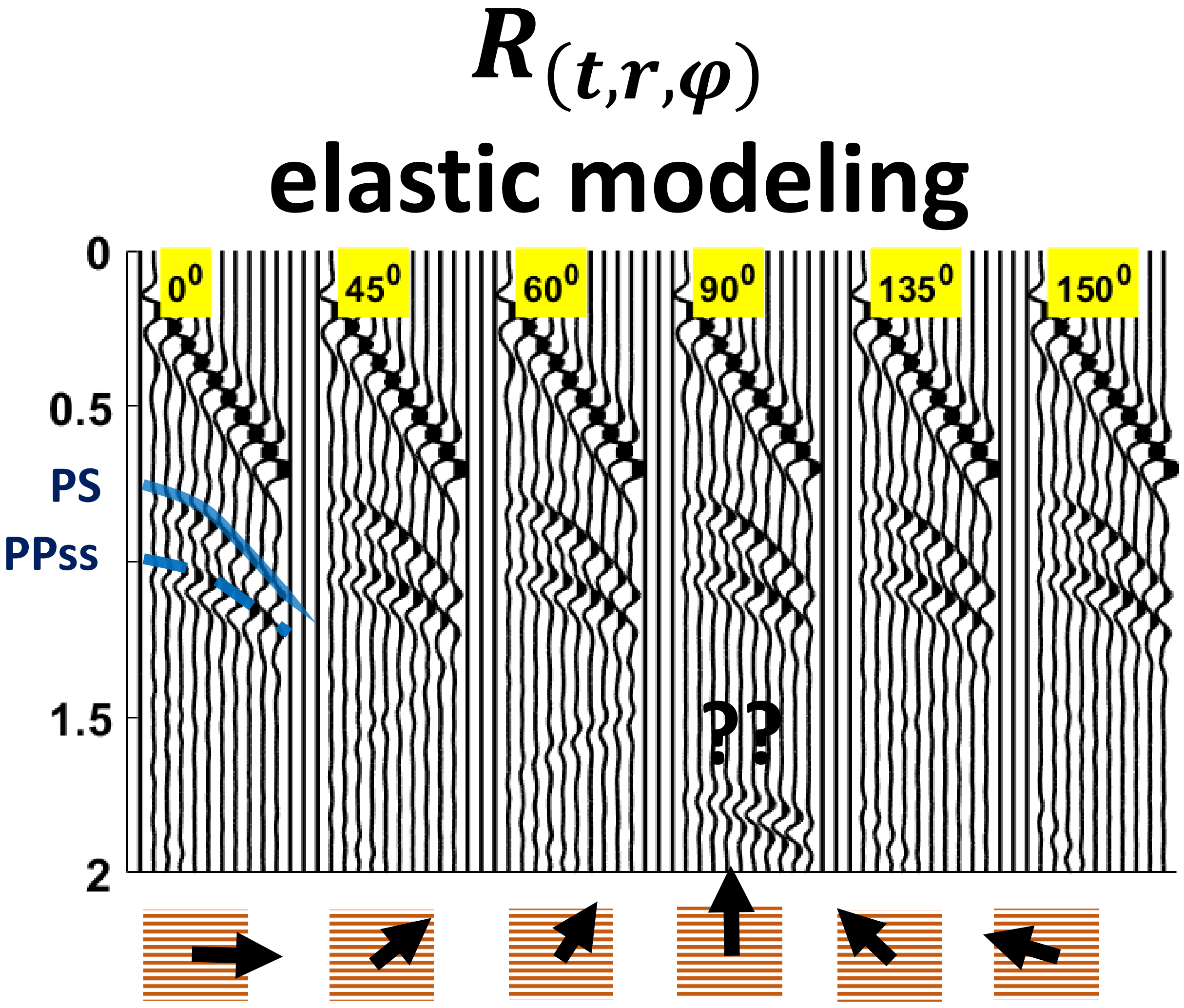

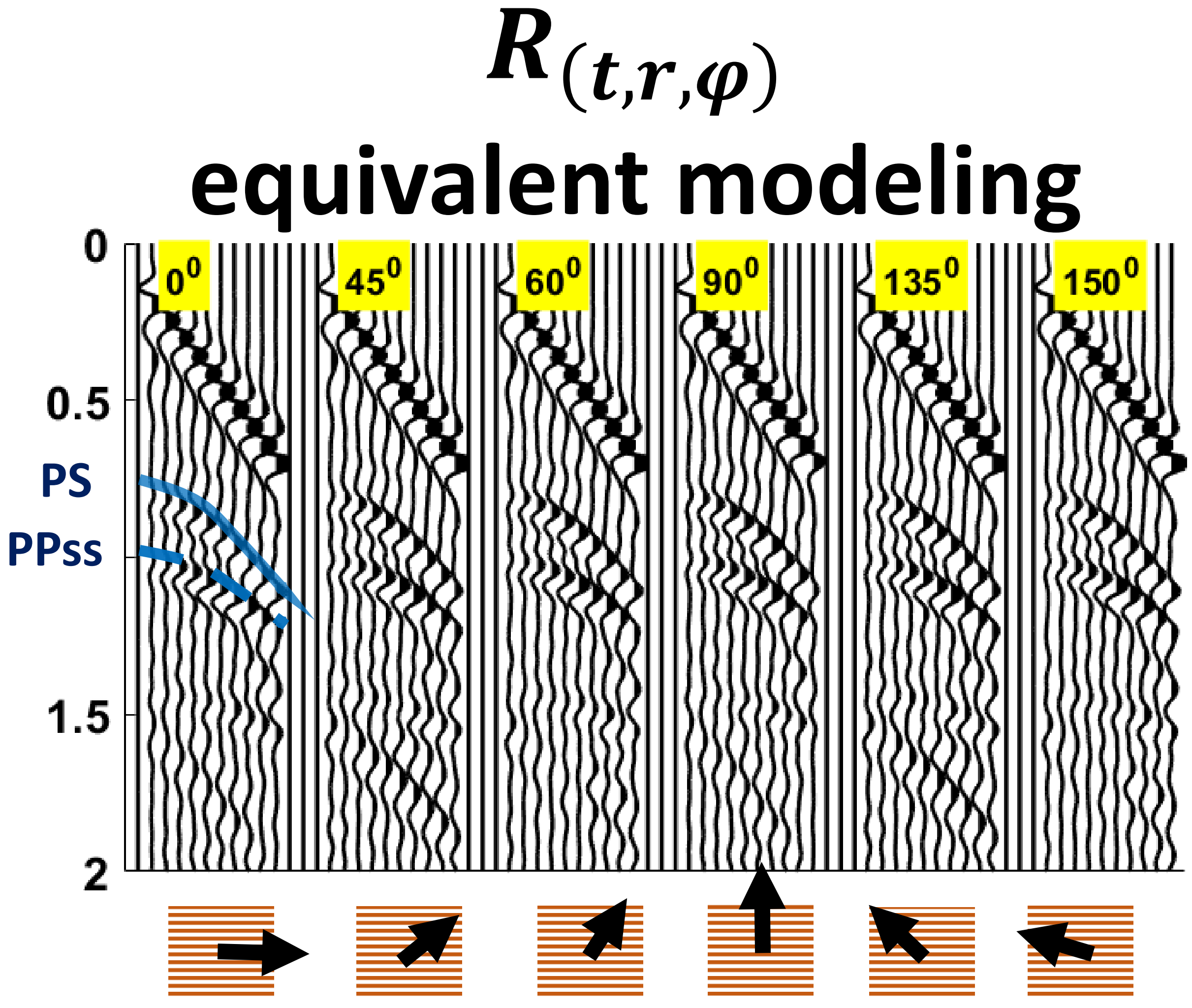

Example: Constant-azimuth Radial Scans

$T_{(t,r,\varphi)}$

elastic modeling

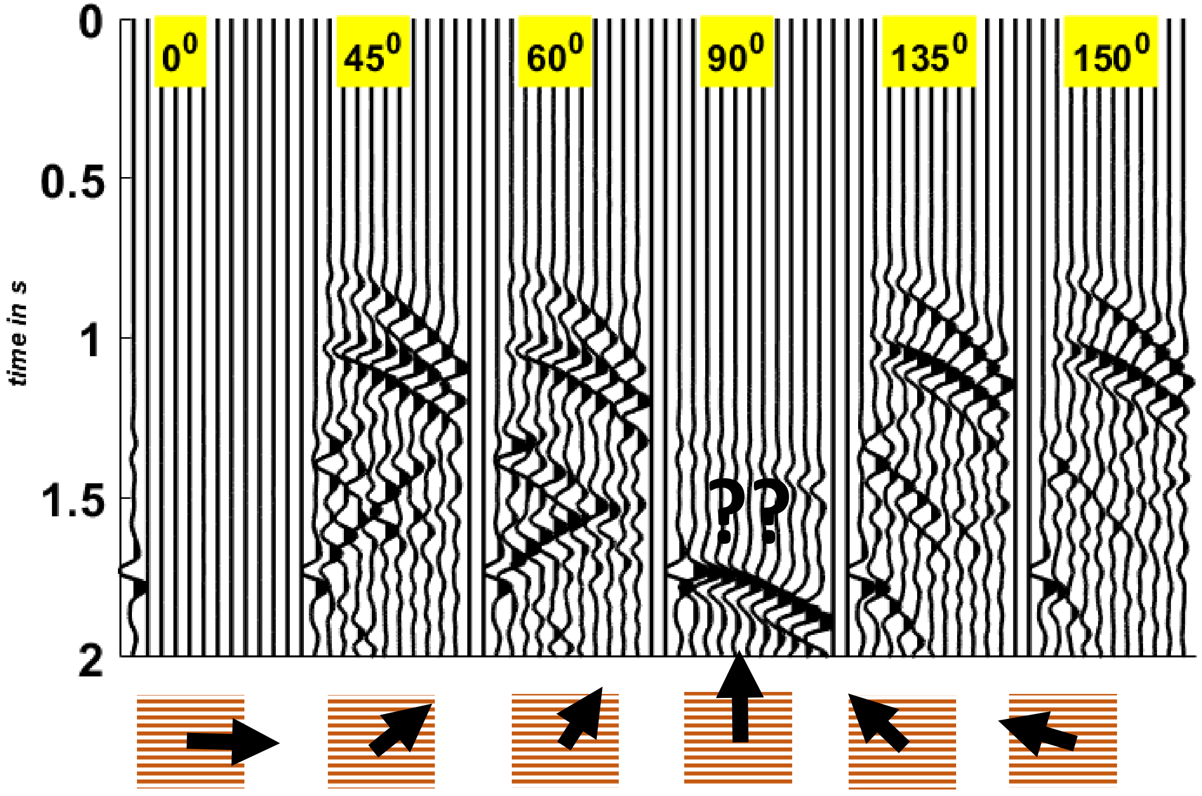

$T_{(t,r,\varphi)}$

equivalent modeling

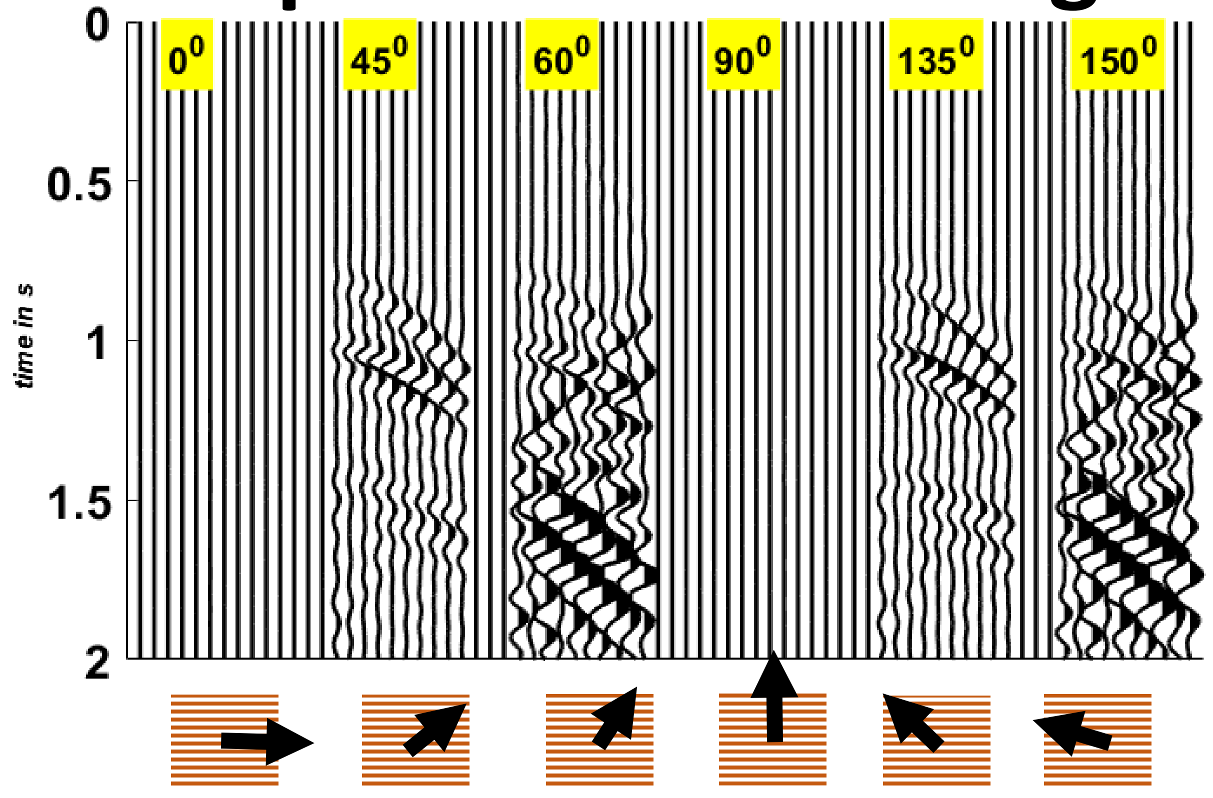

Example: Constant-offset azimuthal scans

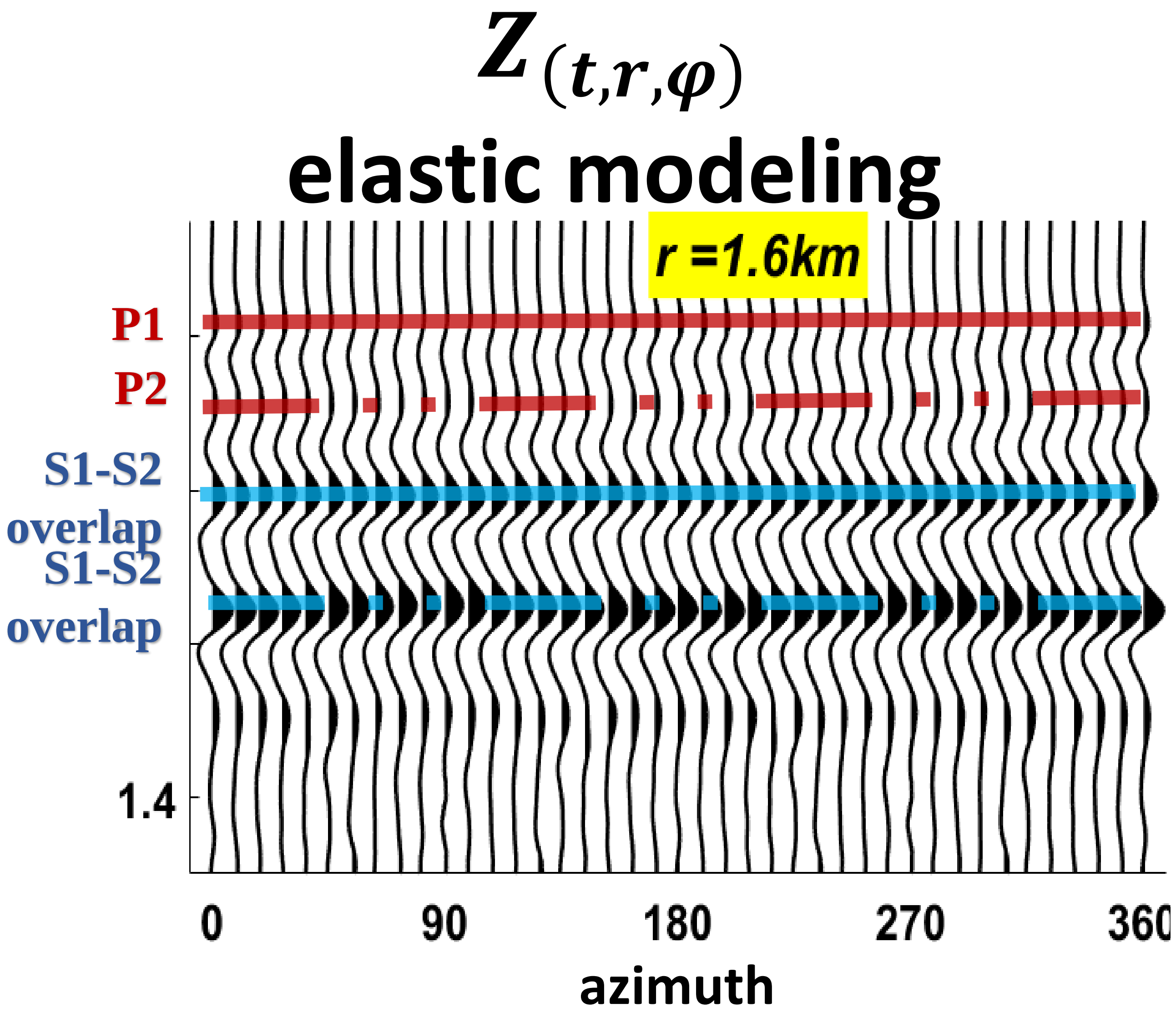

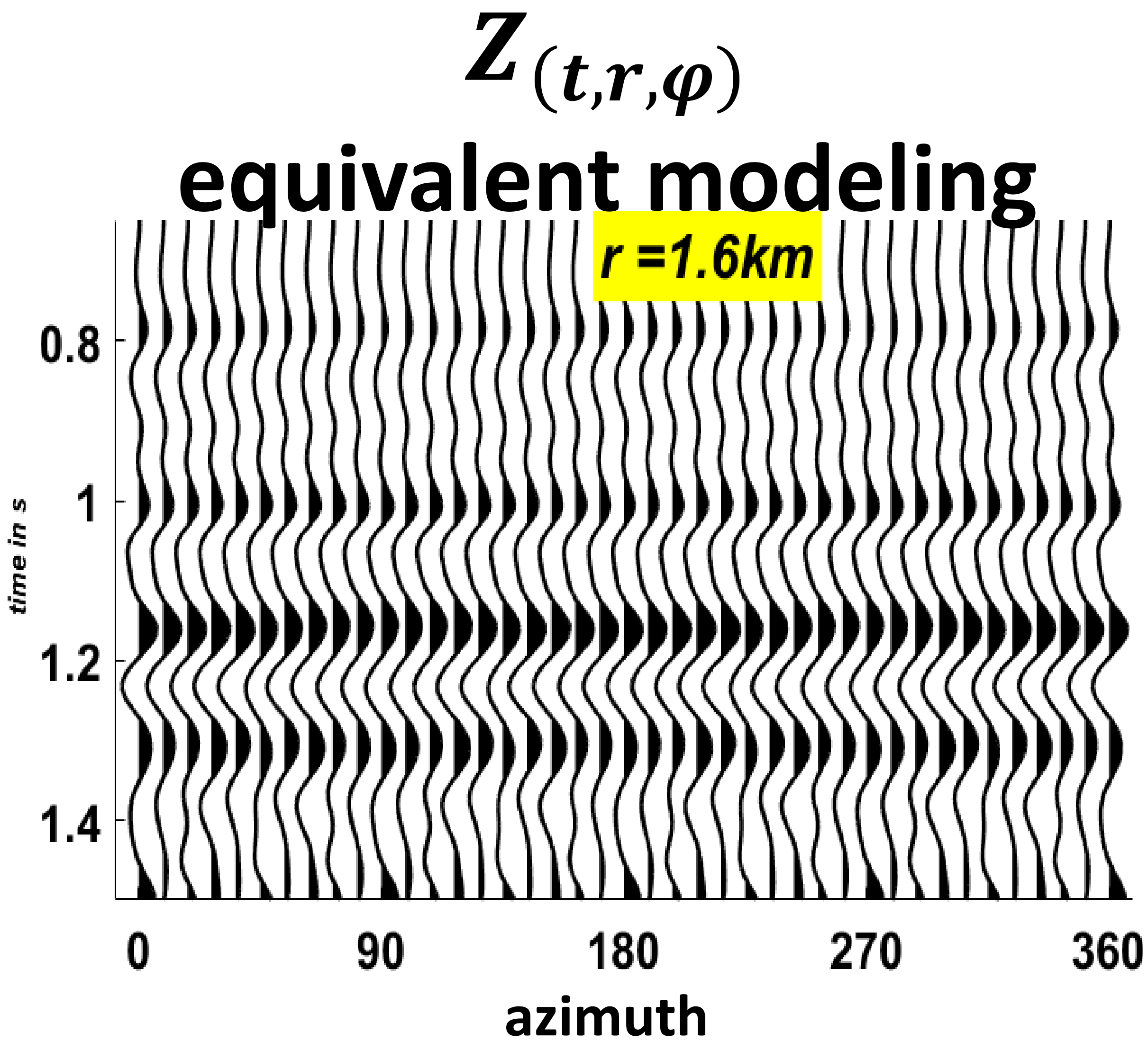

Example : Constant-offset azimuthal scans

$R_{(t,r,\varphi)}$

elastic modeling

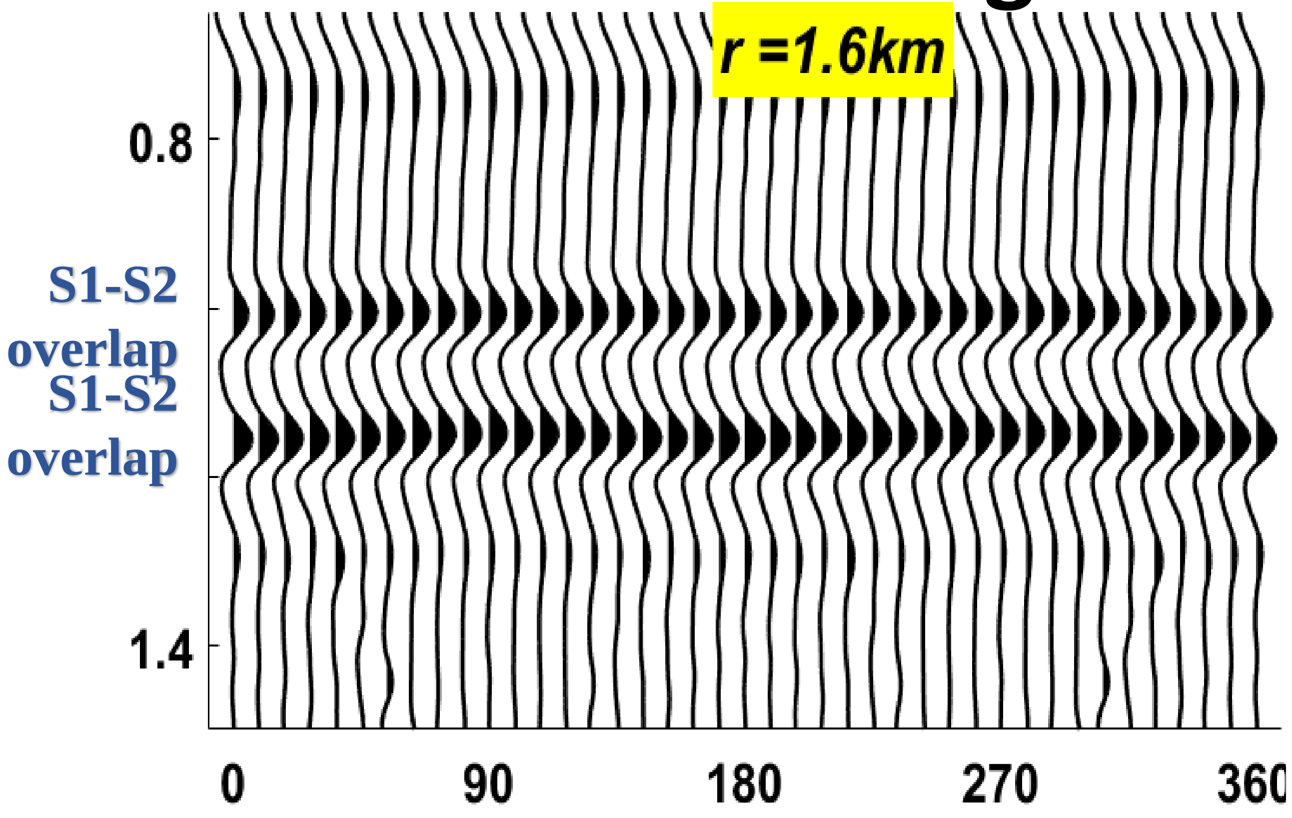

$R_{(t,r,\varphi)}$

equivalent modeling

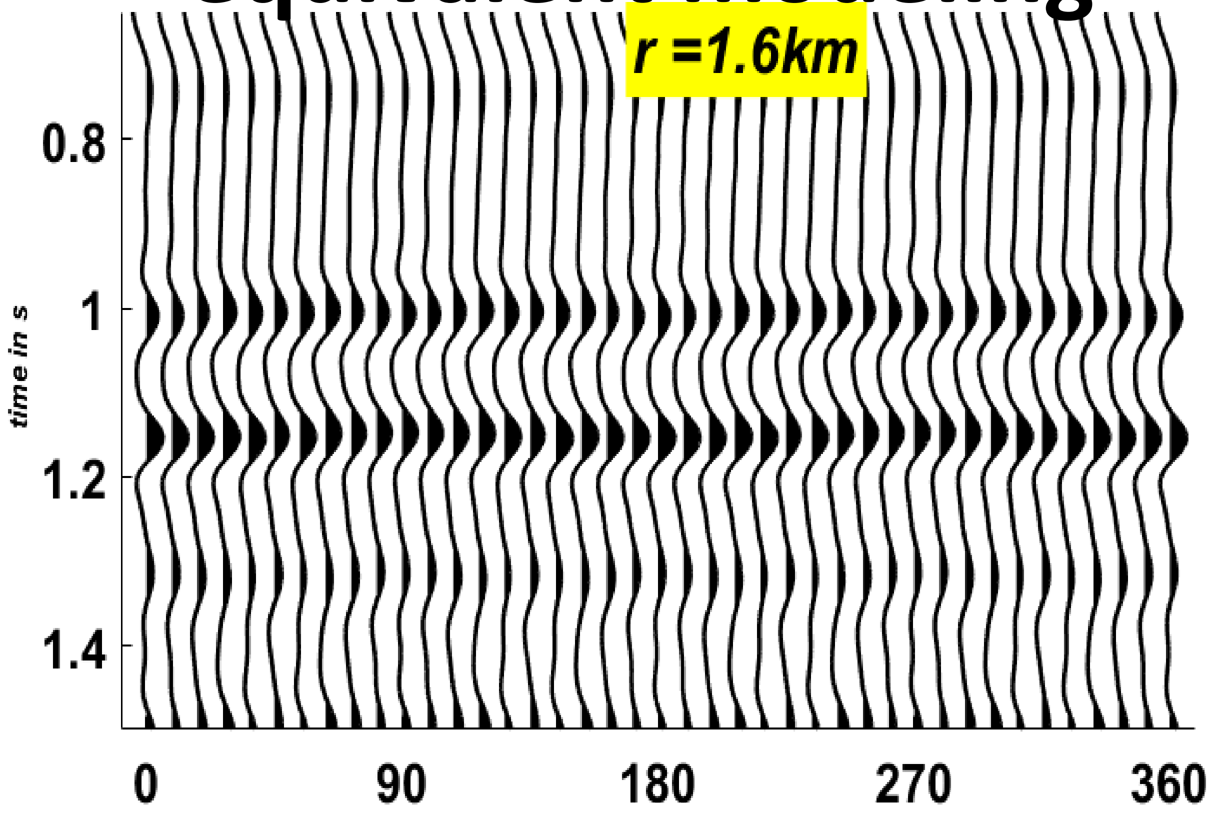

Example : Constant-offset azimuthal scans

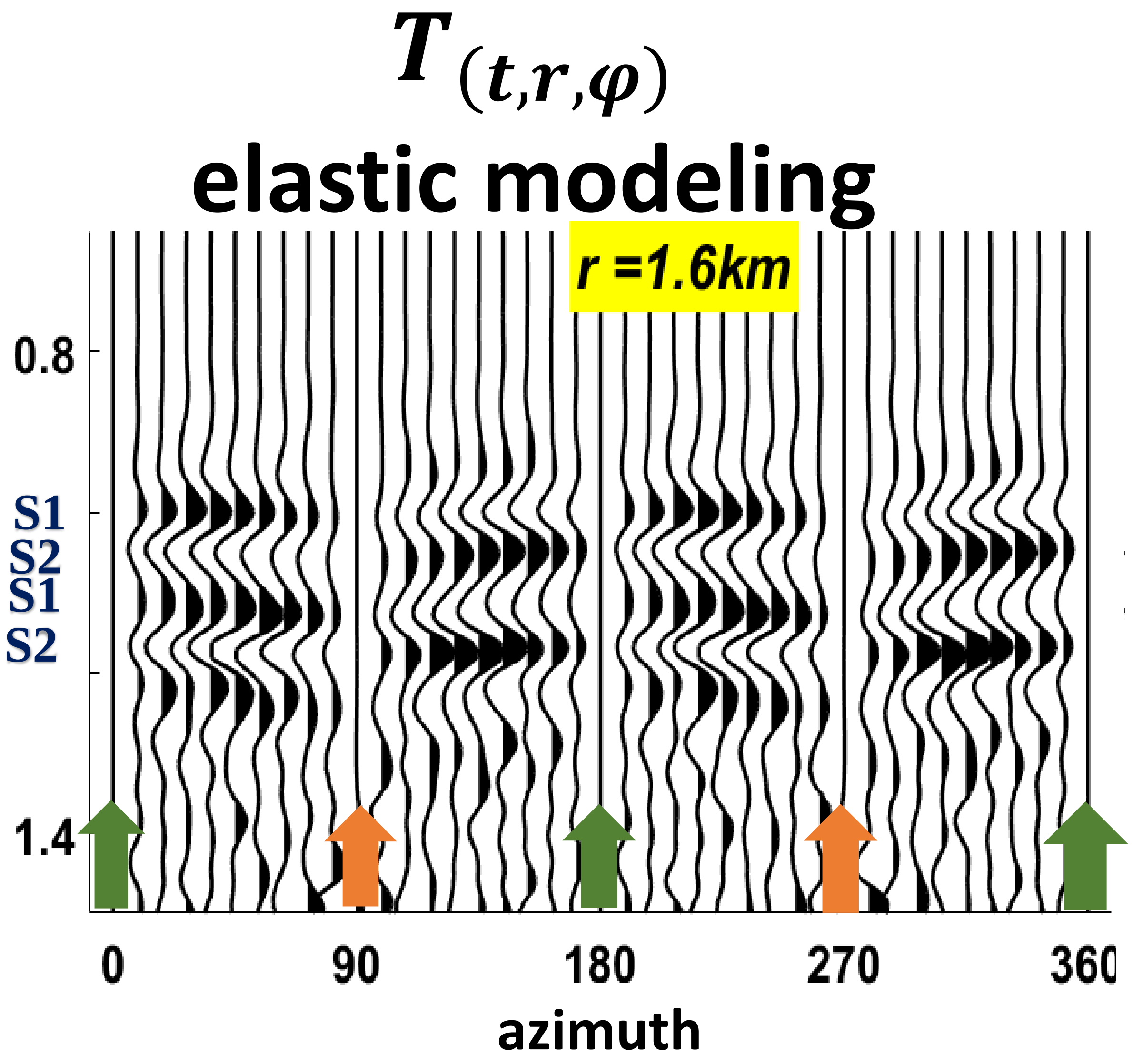

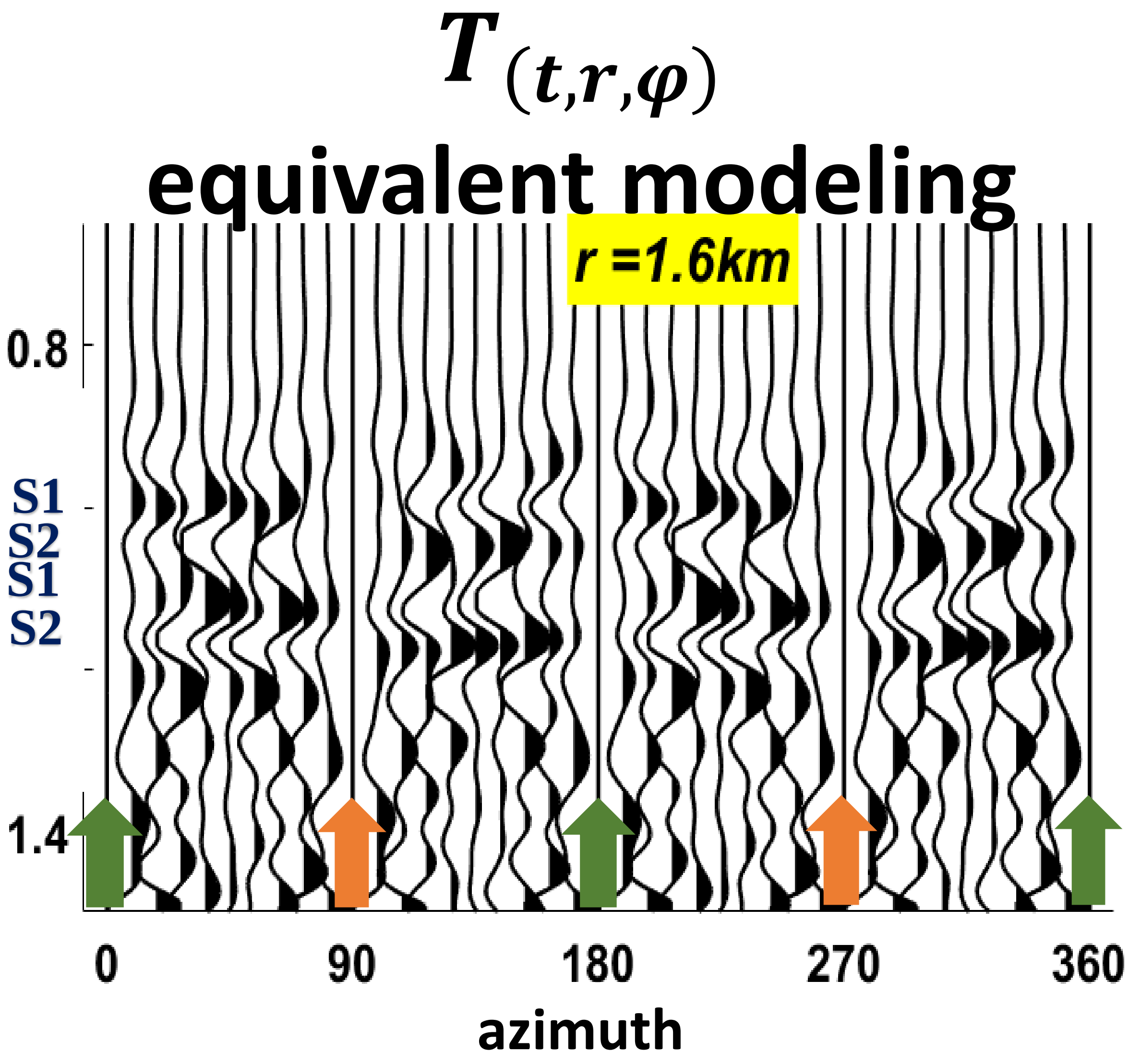

Example: Offset-Azimuth analysis: Top of HTI

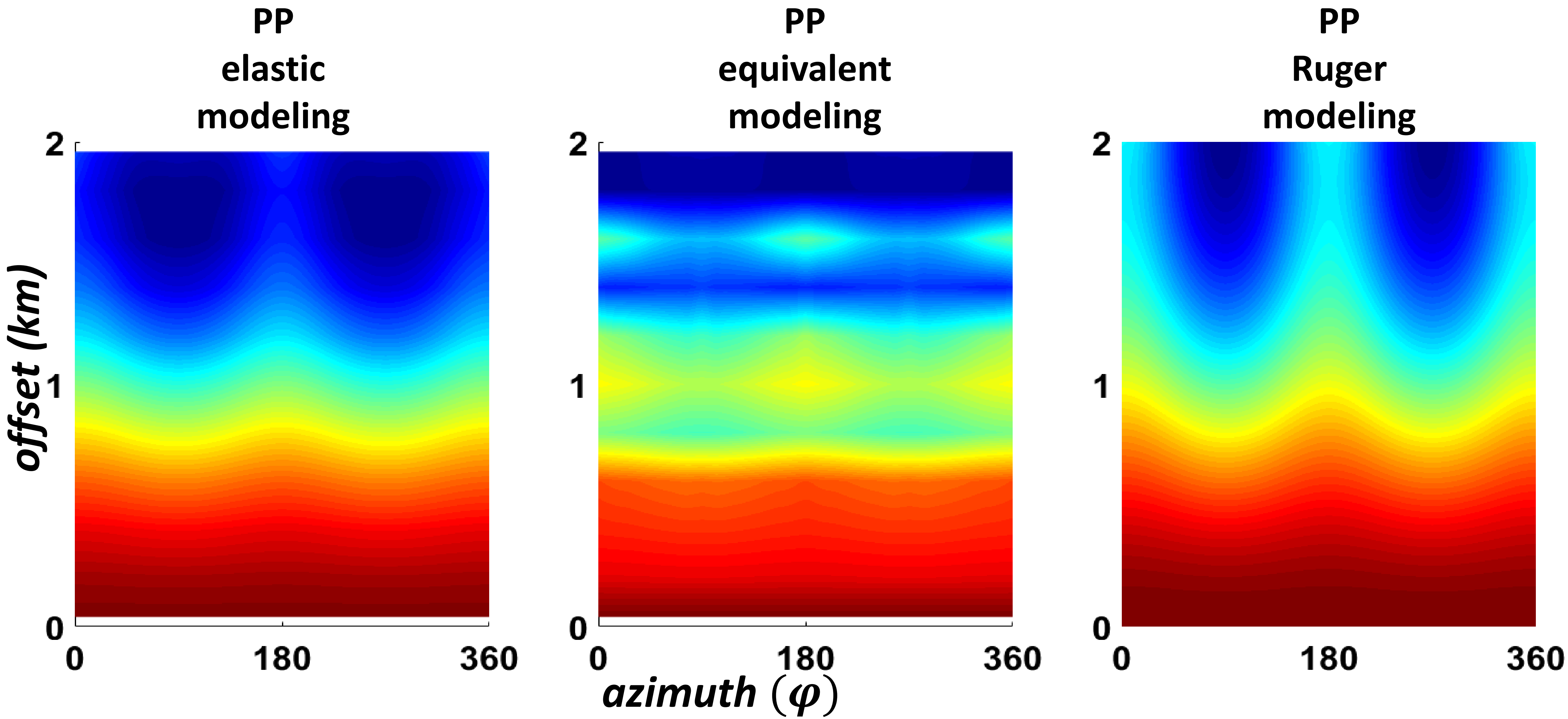

Example: Offset-Azimuth analysis: Top of HTI

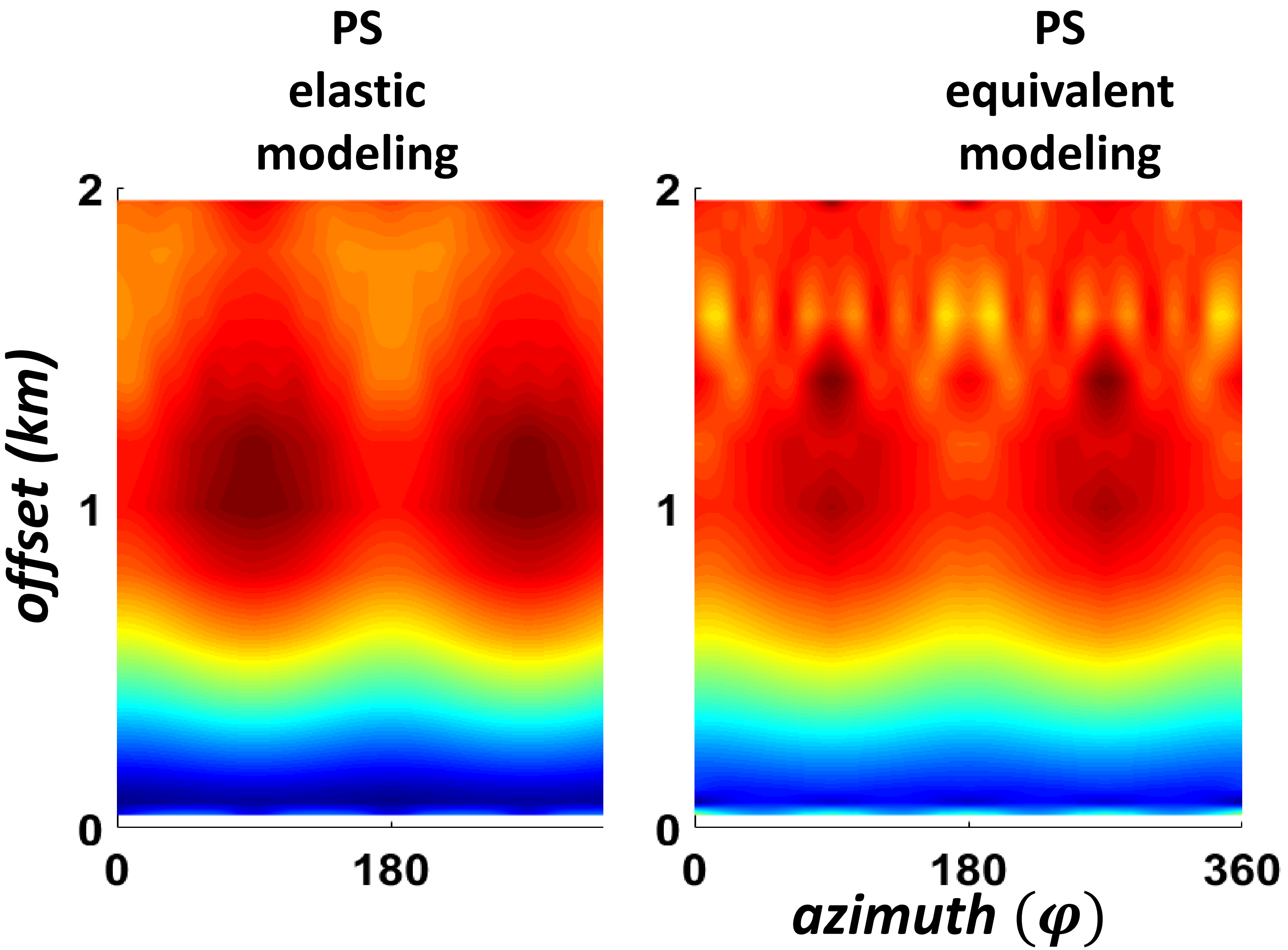

Example: Offset-Azimuth analysis: Top of HTI

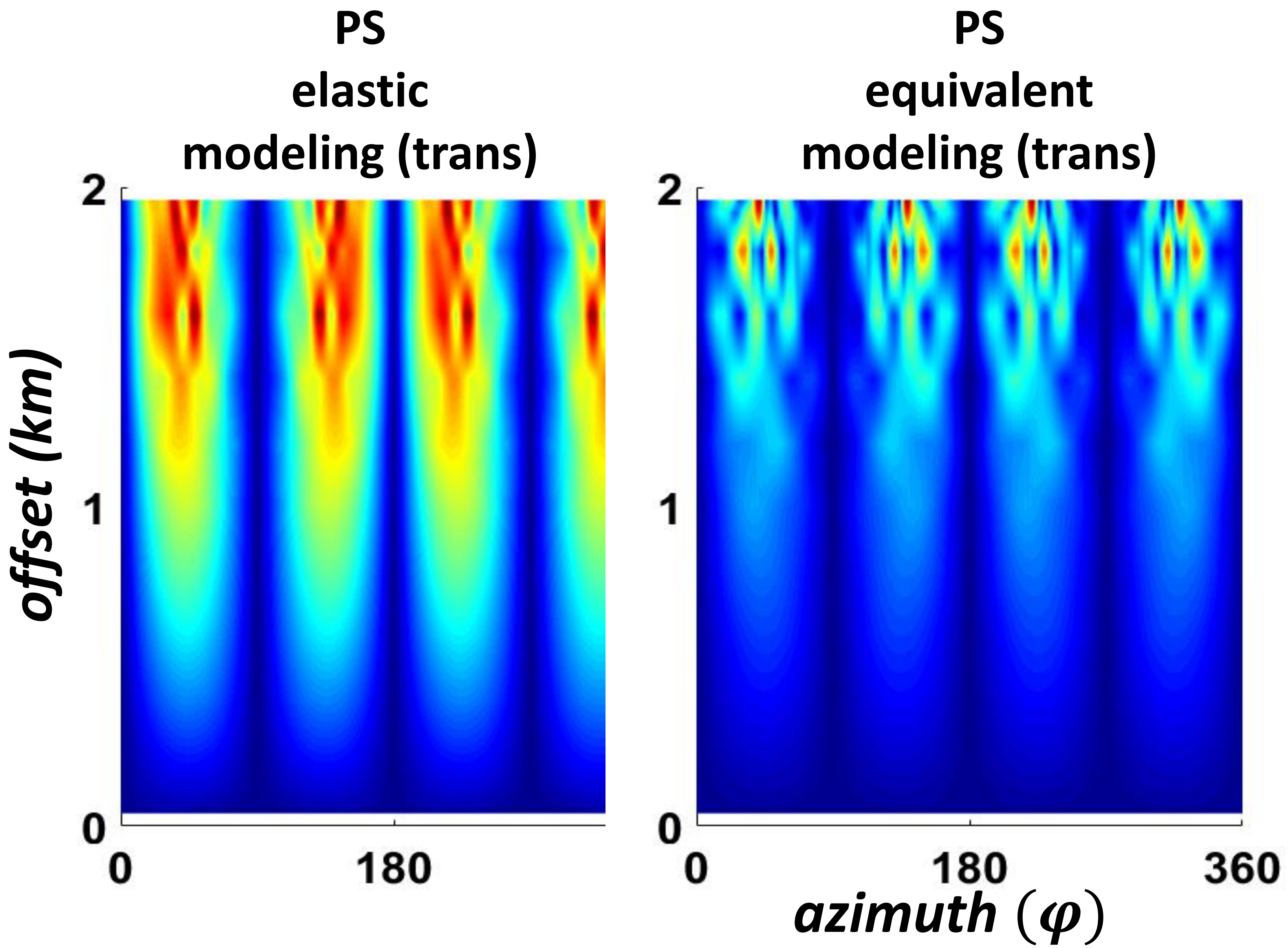

Example: AVAZ analysis, top of HTI

$REFL_{PP}$ ELASTIC MODELING

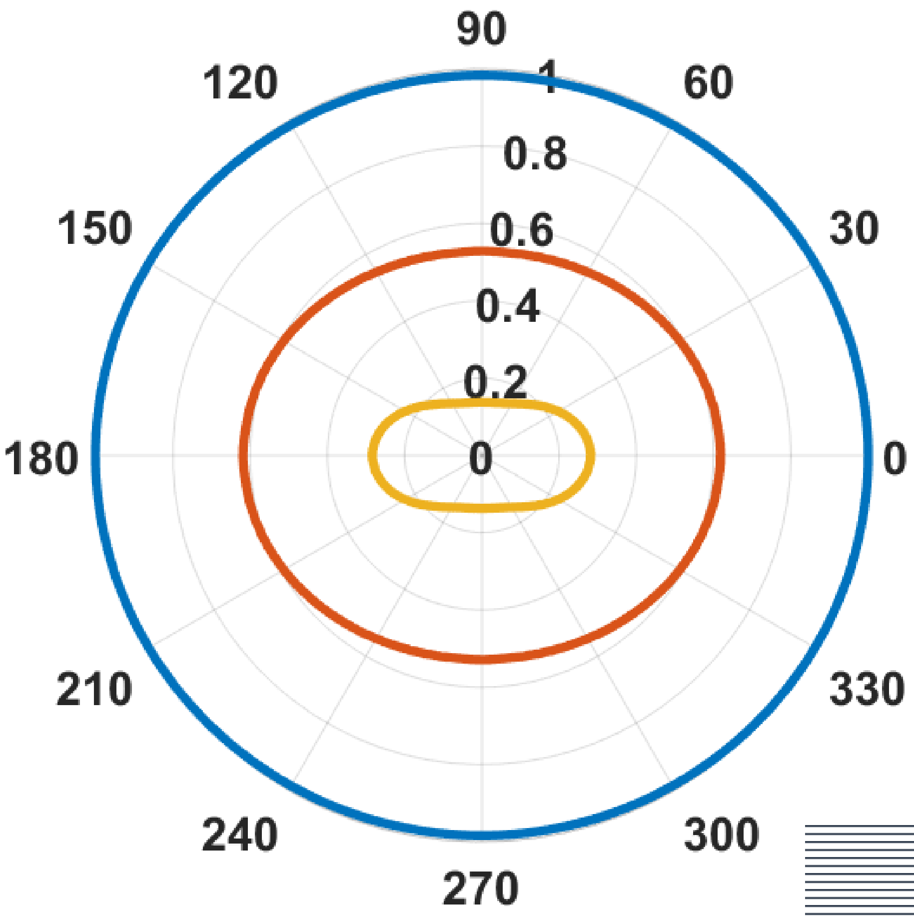

$REFL_{PP}$ EQUIVALENT MODELING

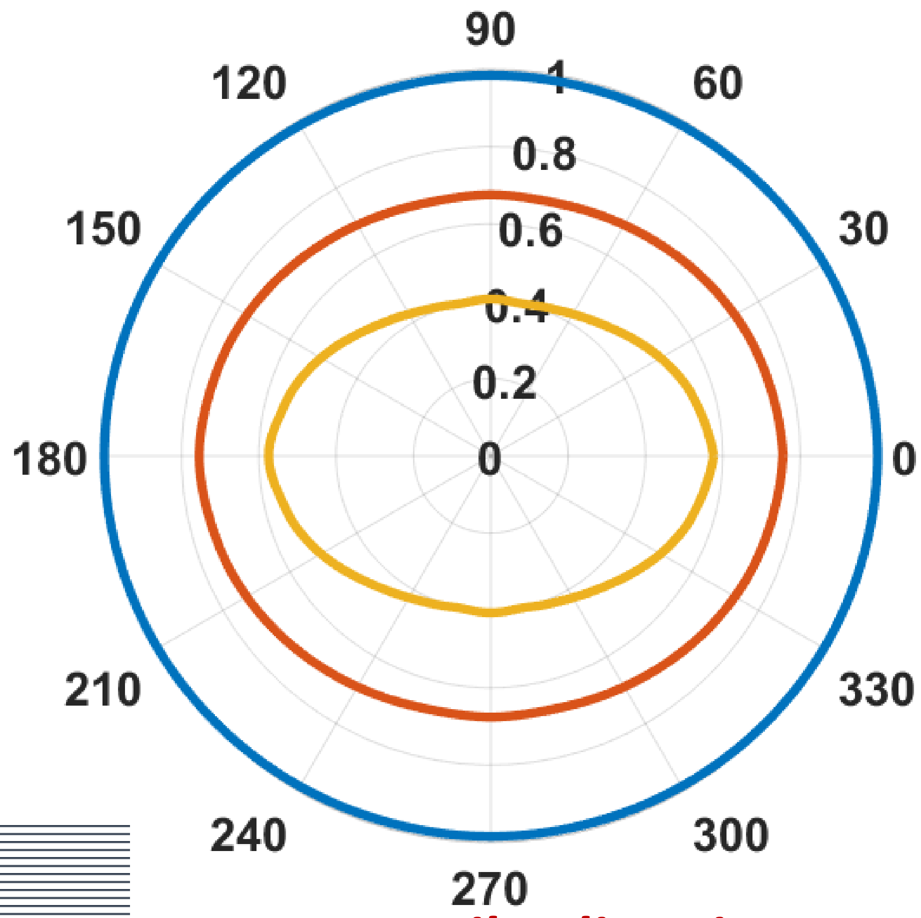

R_{PP} RUGER

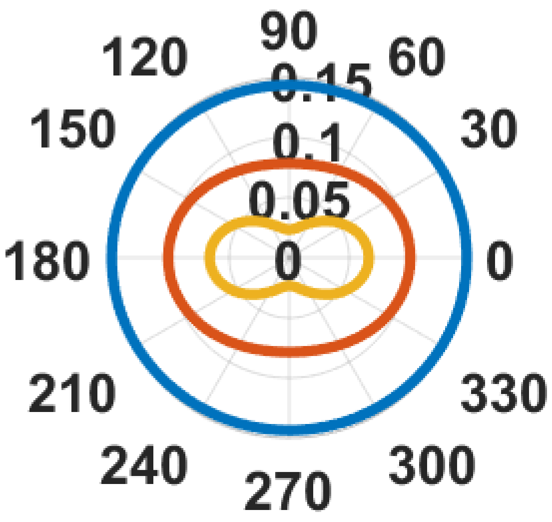

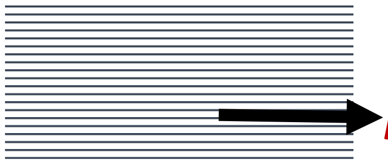

Fracture strike direction

Example: AVAZ analysis elliptical fitting , top of HTI

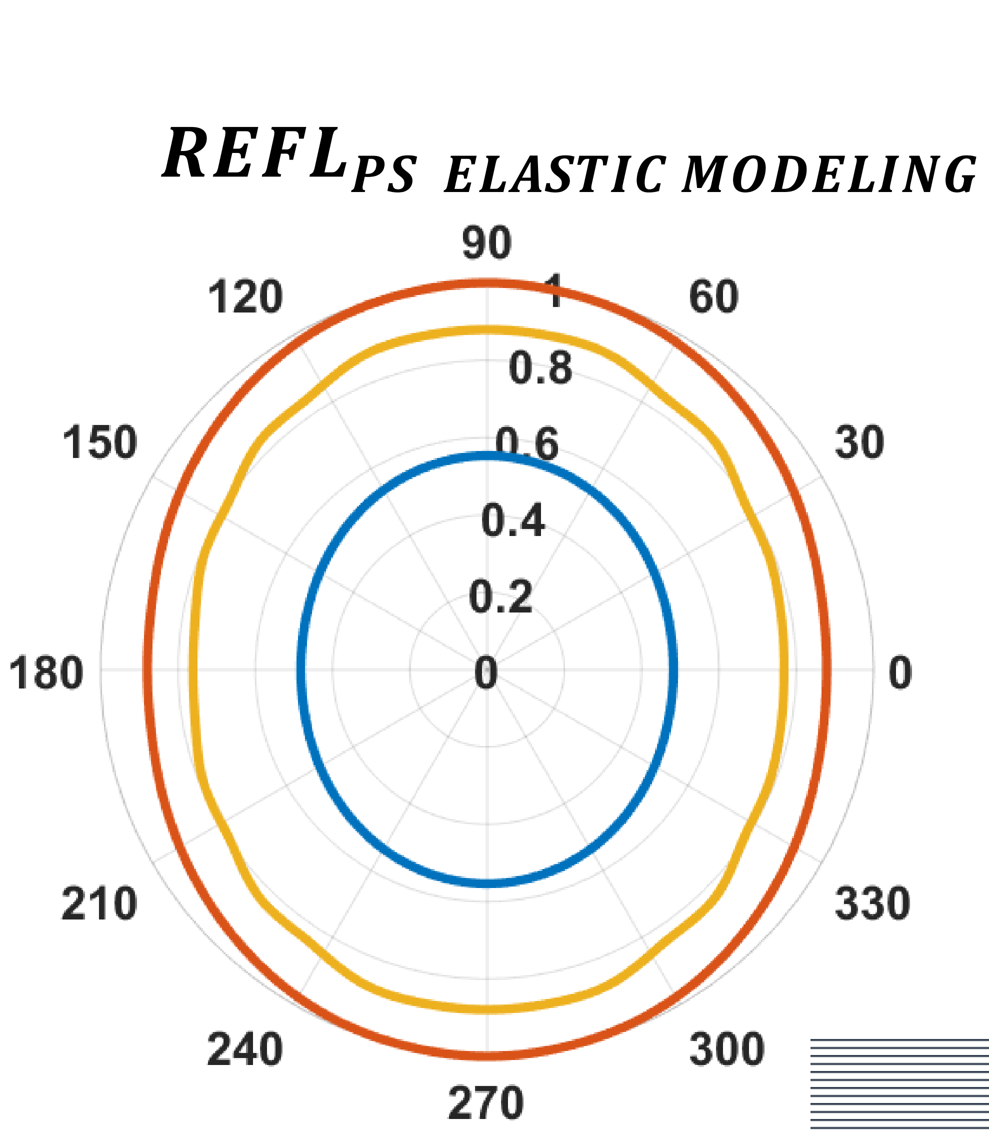

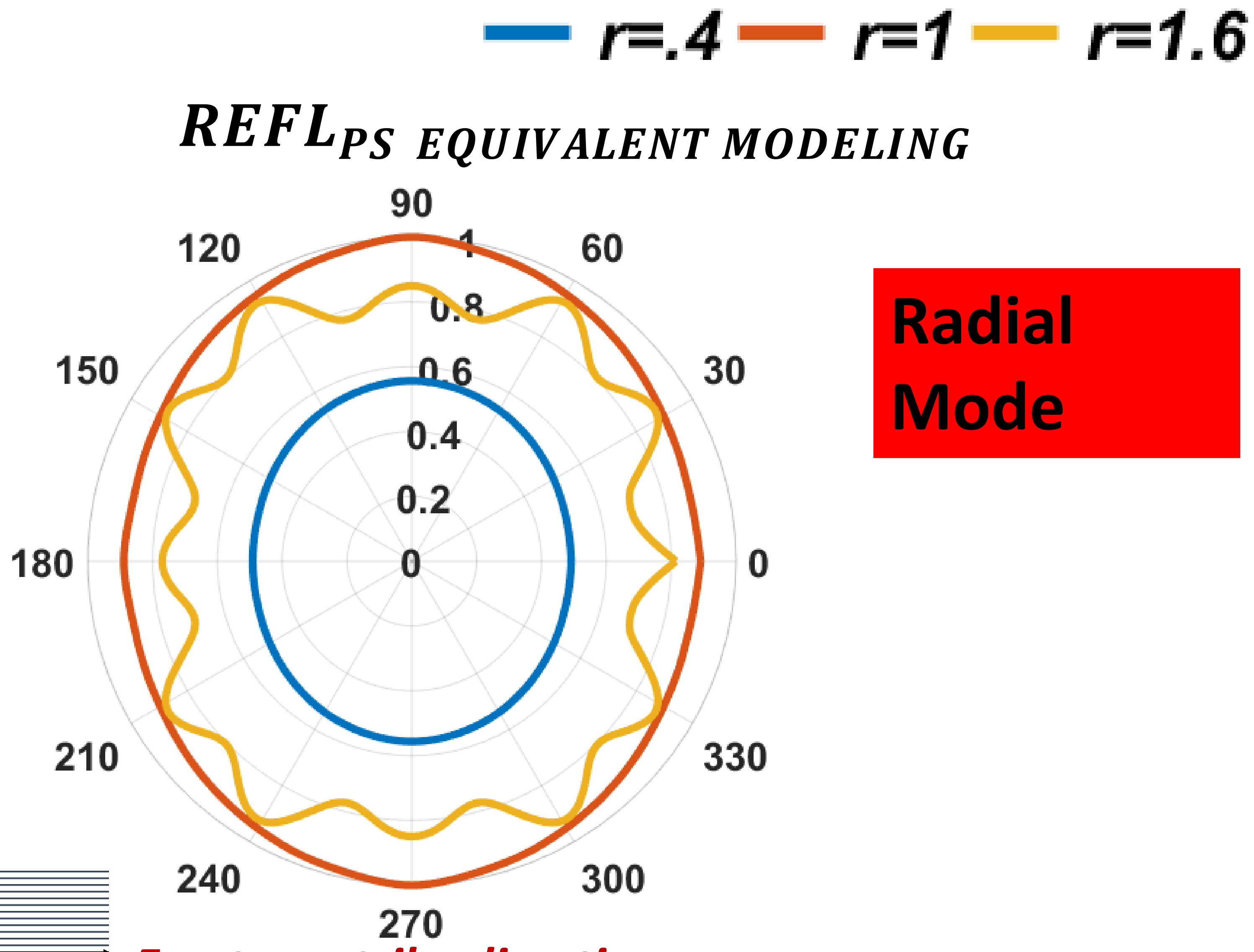

Radial Mode

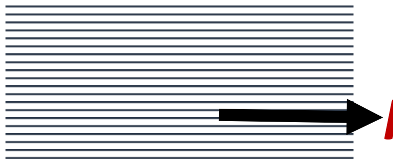

Example: AVAZ analysis elliptical fitting , top of HTI

r=.4 r=1 r=1.6

$REFL_{PS}$ ELASTIC MODELING

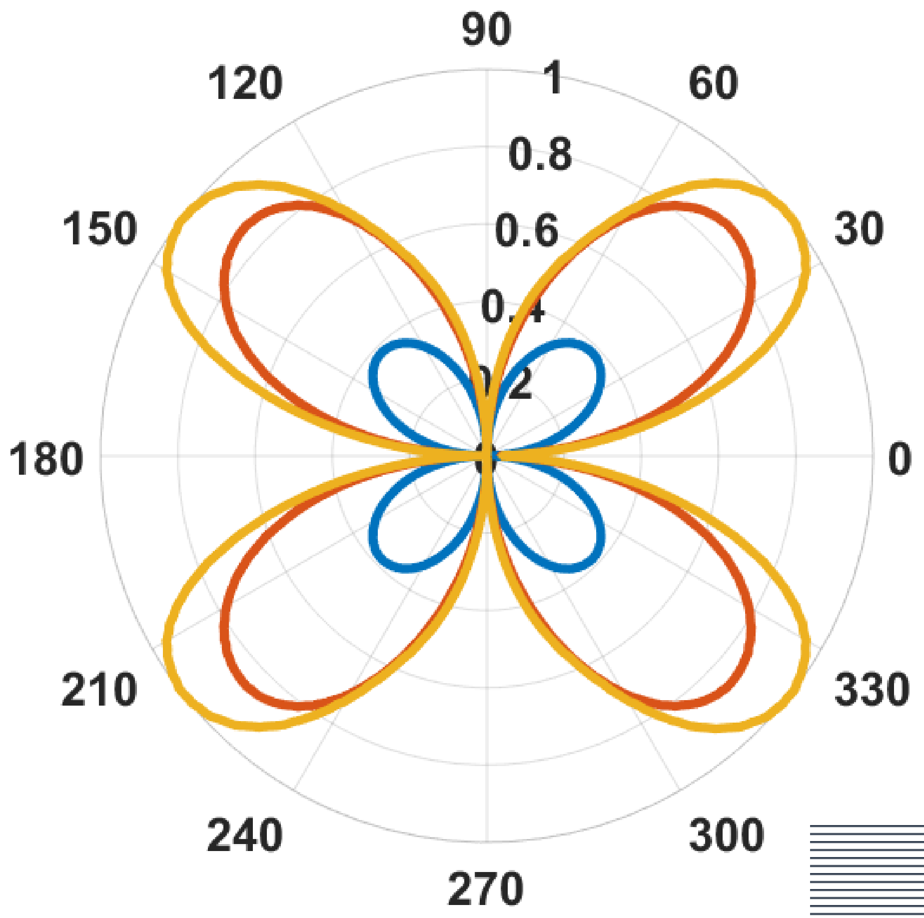

$REFL_{PS}$ EQUIVALENT MODELING

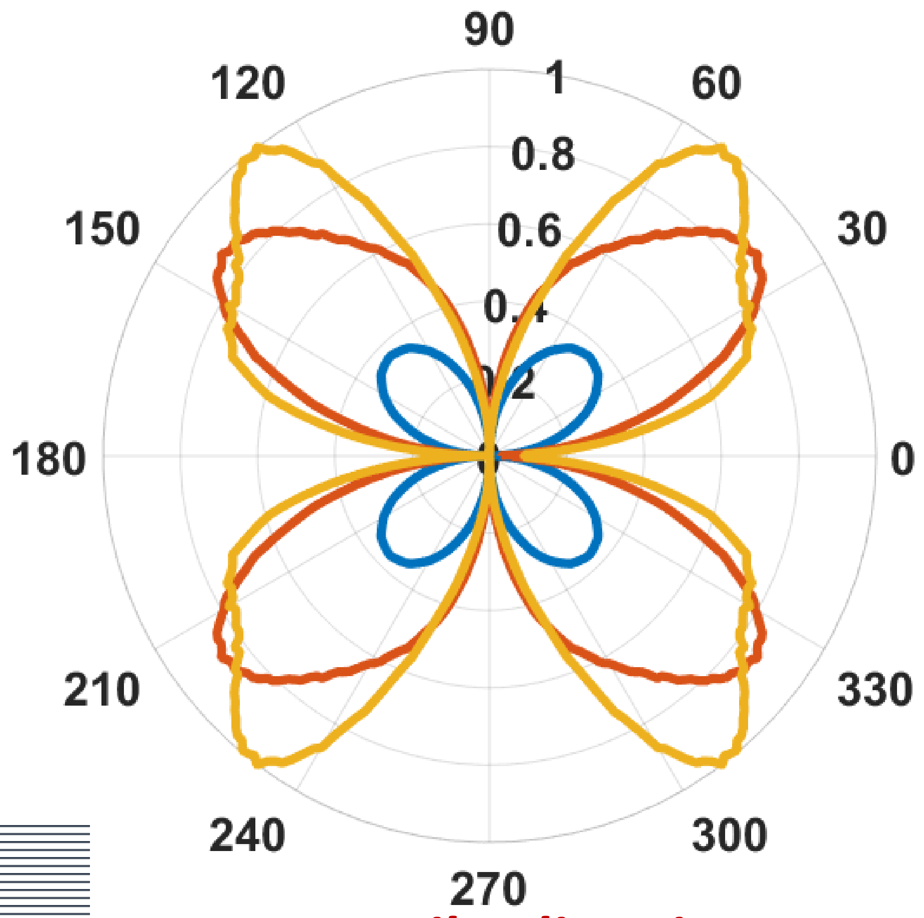

Transverse Mode

Fracture strike direction

Example: interval TVAZ analysis, top-base of HTI

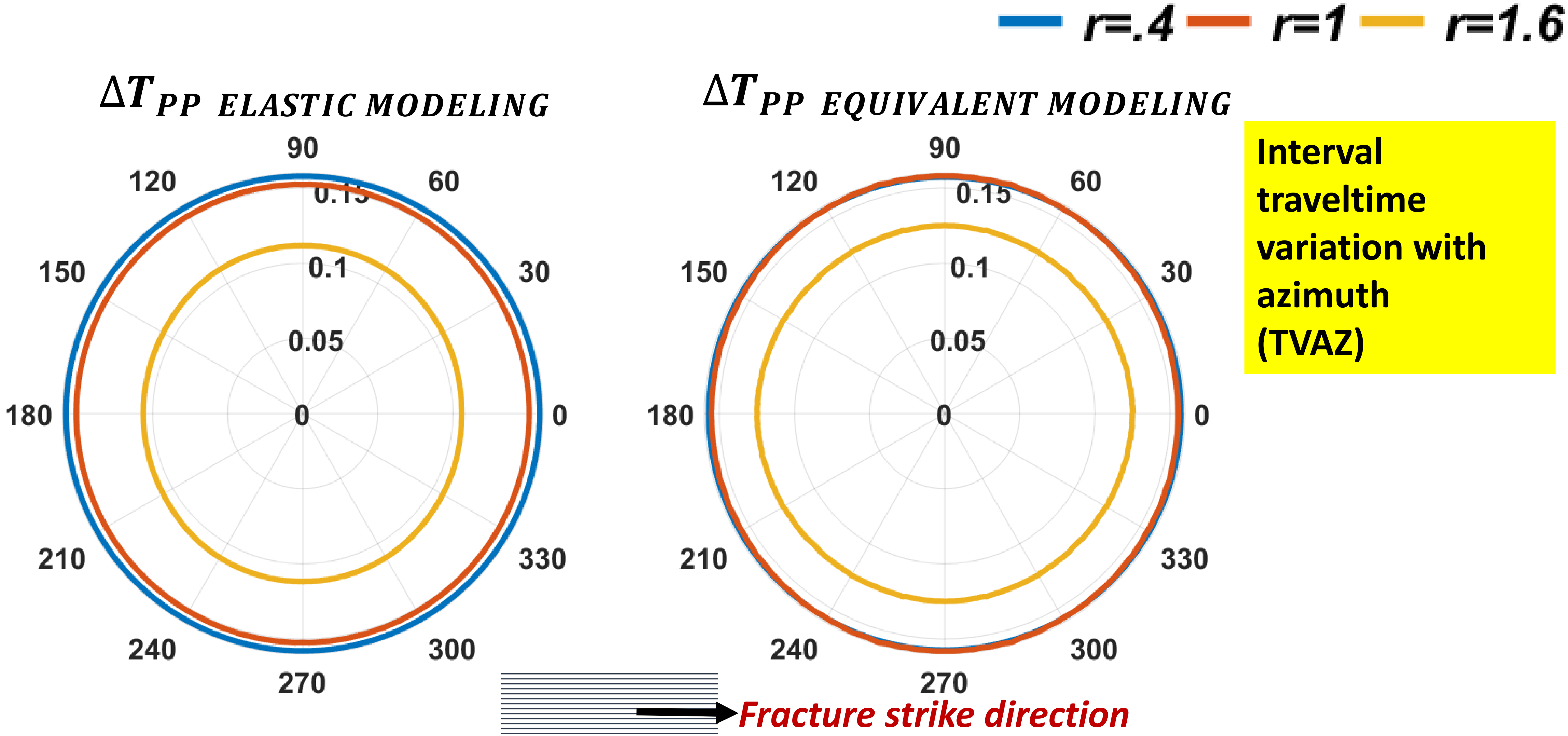

Interval traveltime variation with azimuth (TVAZ)

Example: interval TVAZ analysis, top-base of HTI

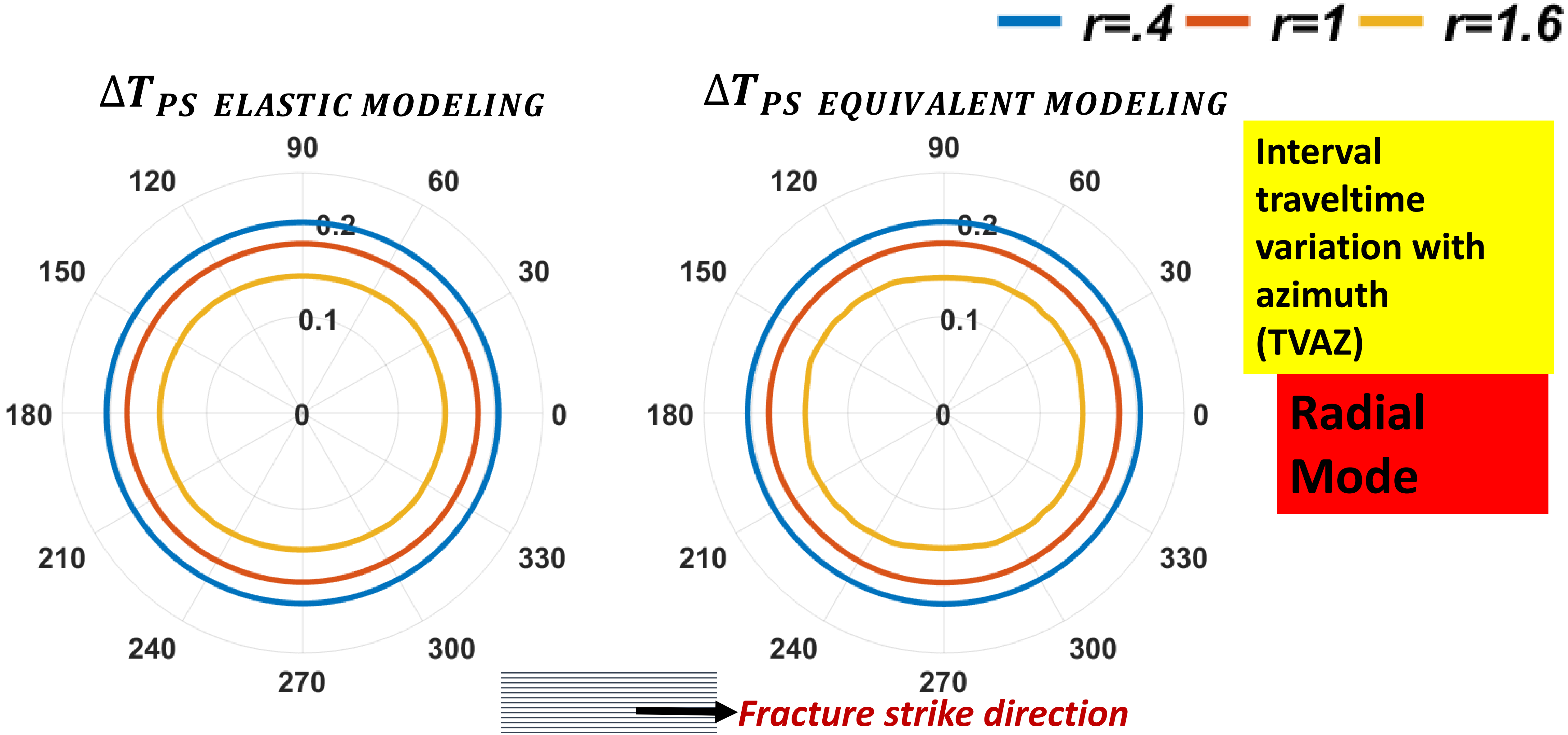

Interval traveltime variation with azimuth (TVAZ)

Radial Mode

Conclusion

- We have demonstrated and compared numerical datasets from elastic and equivalent models.
- We also carried out PP- and PS- AVO, AVAZ and interval TVAZ analysis from elastic and equivalent modeling and compared the P-wave modeling results P-wave results with Ruger modeling.
- We see that the moveout signature and arrival times of the primary PP and PS- events are the same for both models, however the equivalent modeling produce other stronger multimodes.
- We can infer that the quality of P-wave AVO/AVAZ analysis from the analytical Ruger modeling is closer to the elastic modeling than to the finite-difference equivalent modeling.
- Also, the quality of the PS converted AVAZ result for both models was very good. However, the quality of the P-wave modeling is noisier in the equivalent model

Conclusion

- We have also seen that the finite difference elastic modeling generates less noisier multiples and multimodes than the equivalent modeling.
- We can agree that heterogeneous medium produce attenuated multiples and multimodes events because of irregular scattering and layer filtering effect.
- We can conclude that in some circumstances modeling using heterogeneous elastic models might be of higher processing and imaging value than with equivalent media.
- Detailed analysis of the distorted long offset P-wave primary reflections will be objects of further study.

- NSERC: grant CRDPJ 379744-08
- CREWES sponsors
- CREWES staff and students

Thank you

Theory-Schoenberg and Muir (1989)

Carcione (2012) paper on Numerical test on the Schoenberg and Muir theory

Stress-strain relation of individual layers of a layered medium

$$\begin{bmatrix}\sigma_{Ti}\\ \sigma_{N}\end{bmatrix} = \begin{bmatrix} C_{TTi} & C_{TNi} \\ C_{NTi} & C_{NNi}\end{bmatrix}\begin{bmatrix} e_{T} \\ e_{Ni}\end{bmatrix}$$

$\boldsymbol{\sigma_{Ti}}$ and $\boldsymbol{e_T}$ are the in-plane or tangential stress and strain

$\boldsymbol{\sigma_N}$ and $\boldsymbol{e_{Ni}}$ are the cross-plane or normal stress and strain

$\boldsymbol{C_{TTi}}$, $\boldsymbol{C_{NNi}}$, $\boldsymbol{C_{TNi}}$ ***and*** $\boldsymbol{C_{NTi}}$, are 3 x 3 stiffness submatrices denoting stiffness of individual layer

The long-wavelength equivalent homogeneous medium have average stiffness =

$$\begin{bmatrix} \overline{C_{TT}} & \overline{C_{TN}} \\ \overline{C_{TN}}^{\dagger} & \overline{C_{NN}} \end{bmatrix}$$

Theory-Schoenberg and Muir (1989)

Carcione (2012) paper on Numerical test on the Schoenberg and Muir theory

Stress-strain relation of ***individual layers*** ***of a layered medium***

$$\begin{bmatrix} \sigma_{1i} \\ \sigma_{2i} \\ \sigma_{6i} \\ \sigma_{3} \\ \sigma_{4} \\ \sigma_{5} \end{bmatrix} = \begin{bmatrix} C_{11i} & C_{12i} & C_{16i} & C_{13i} & C_{14i} & C_{15i} \\ C_{12i} & C_{22i} & C_{26i} & C_{23i} & C_{24i} & C_{25i} \\ C_{16i} & C_{26i} & C_{66i} & C_{36i} & C_{46i} & C_{56i} \\ C_{13i} & C_{23i} & C_{36i} & C_{33i} & C_{34i} & C_{35i} \\ C_{14i} & C_{24i} & C_{46i} & C_{34i} & C_{44i} & C_{45i} \\ C_{15i} & C_{25i} & C_{56i} & C_{35i} & C_{45i} & C_{55i} \end{bmatrix} \begin{bmatrix} e_{1} \\ e_{2} \\ e_{6} \\ e_{3i} \\ e_{4i} \\ e_{5i} \end{bmatrix}$$

$$\begin{bmatrix} \sigma_{Ti} \\ \sigma_{N} \end{bmatrix} = \begin{bmatrix} C_{TTi} & C_{TNi} \\ C_{NTi} & C_{NNi} \end{bmatrix} \begin{bmatrix} e_{T} \\ e_{Ni} \end{bmatrix}$$

The long-wavelength equivalent homogeneous medium have ***average stiffness***

$$= \begin{bmatrix} \overline{C}_{TT} & \overline{C}_{TN} \\ \overline{C}_{TN}^{\dagger} & \overline{C}_{NN} \end{bmatrix}$$

The new stress strain relation for homogeneous equivalent medium

$$= \begin{aligned} \langle \sigma_T \rangle &= \overline{C}_{TT}\, e_T + \overline{C}_{TN} \langle e_N \rangle \\ \sigma_N &= \overline{C}_{TN}^{\dagger}\, e_T + \overline{C}_{NN} \langle e_N \rangle \end{aligned}$$

$$\overline{C}_{NN} = \langle \overline{C}_{NN}^{-1} \rangle^{-1},$$

$$\overline{C}_{TN} = \langle C_{TN} C_{NN}^{-1} \rangle \overline{C}_{NN},$$

$$\overline{C}_{TT} = \langle C_{TT} \rangle - \langle C_{TN} C_{NN}^{-1} C_{NT} \rangle + \overline{C}_{TN} \langle \overline{C}_{NN}^{-1} C_{NT} \rangle,$$

where $\langle C \rangle = \sum_{i=1}^{N} H_i C_i$

Theory-Schoenberg and Muir (1989)

Average stiffness and fracture parameter estimation

$$C^e_{33} = \langle\frac{1}{C_{33}}\rangle^{-1},$$

$$C^e_{44} = C^e_{55} = \langle\frac{1}{C_{44}}\rangle^{-1},$$

$$C^e_{13} = C^e_{23} = \langle\frac{C_{12}}{C_{33}}\rangle\langle\frac{1}{C_{33}}\rangle^{-1},$$

$$C^e_{66} = C_{66},$$

$$C^e_{11} = C^e_{22} = \langle C_{11}\rangle + \langle\frac{C_{12}}{C_{33}}\rangle^2\langle\frac{1}{C_{33}}\rangle^{-1} - \langle\frac{C^2_{12}}{C_{33}}\rangle$$

$$C^e_{12} = \langle C_{12}\rangle + \langle\frac{C_{12}}{C_{33}}\rangle^2\langle\frac{1}{C_{33}}\rangle^{-1} - \langle\frac{C^2_{12}}{C_{33}}\rangle = C^e_{11} - 2C^e_{66}\ .$$

Elasticity matrix of HTI from rotated VTI

$$\begin{pmatrix} c_{11} & c_{12} & c_{13} & 0 & 0 & 0 \\ c_{12} & c_{11} & c_{13} & 0 & 0 & 0 \\ c_{13} & c_{13} & c_{33} & 0 & 0 & 0 \\ 0 & 0 & 0 & c_{55} & 0 & 0 \\ 0 & 0 & 0 & 0 & c_{55} & 0 \\ 0 & 0 & 0 & 0 & 0 & c_{66} \end{pmatrix} \rightarrow \begin{pmatrix} c_{33} & c_{13} & c_{13} & 0 & 0 & 0 \\ c_{13} & c_{11} & c_{12} & 0 & 0 & 0 \\ c_{13} & c_{12} & c_{11} & 0 & 0 & 0 \\ 0 & 0 & 0 & c_{66} & 0 & 0 \\ 0 & 0 & 0 & 0 & c_{55} & 0 \\ 0 & 0 & 0 & 0 & 0 & c_{55} \end{pmatrix}$$

VTI stiffness matrix — **HTI matrix from VTI rotation**

Thomsen-style anisotropic parameter estimation for finite-difference modeling

$$V_{p0} = \sqrt{C_{33}/\rho},$$

$$V_{s0} = \sqrt{C_{55}/\rho},$$

$$\varepsilon^v = (C_{33} - C_{11})/2C_{11},$$

$$\gamma^v = (C_{44} - C_{55})/C_{55},$$

$$\delta^v = ((C_{13} + C_{55})^2 - (C_{33} - C_{55})^2)/2C_{55},$$

$$Vs_{slow} = V_{so} = \sqrt{C_{55}/\rho},$$

$$Vs_{fast} = \sqrt{C_{44}/\rho} \approx V_{so}(1 + \gamma^v)$$